The Institute of Paper Chemistry

Appleton, Wisconsin

Doctor's Dissertation

The Transverse Tensile Strength of Clay-Starch Coatings as a Function of Adhesive Distribution

Arnold Charles Eames

June, 1959

THE TRANSVERSE TENSILE STRENGTH OF CLAY-STARCH COATINGS AS A FUNCTION OF ADHESIVE DISTRIBUTION

A thesis submitted by

Arnold Charles Eames

B.M.E. 1951, Rensselaer Polytechnic Institute
M.S. 1956, Lawrence College

in partial fulfillment of the requirements
of The Institute of Paper Chemistry
for the degree of Doctor of Philosophy
from Lawrence College,
Appleton, Wisconsin

June, 1959

TABLE OF CONTENTS

A NEW APPROACH TO COATING STRENGTH

The most important strength criterion in pigment-coated printing papers is a property called pick strength. Pick strength may be defined as the resistance of paper to the removal of coating or fibers or to cleavage parallel to the sheet direction when the paper is printed. The stresses primarily responsible for failure during printing are generally believed to arise in the splitting of tacky ink films. Evaluation of coating strength has been directed largely at methods that give results in line with the performance of the coated paper on the printing press. The development in this direction of end-use evaluation has proceeded to the point that actual presses are sometimes used to test the strength of coated papers. A refinement of this approach is embodied in the tests that utilize printing stresses.

Tests that utilize printing stresses vary a great deal in design, but all apply stresses to the coated paper by the splitting of a film of ink or other viscous liquid. Notable developments are the IPC bonding strength tester (1,2) and the IGT printability tester (3,4) both of which give results in terms of the viscosity-velocity product (VVP) of the splitting viscous film causing rupture. Other press simulation tests are the LTF pick tester (5), the Warren MP tester (6), the Hercules print tester (7), the Davidson-Pomper pick tester (8), and the rotary pick tester described by Roehr (9).

From the early days of the use of coated papers for printing there have been attempts to evaluate pick strength by means that are quicker,

simpler, and less costly than actually printing samples of the paper. In general, such means have been used by experienced personnel only as a guide and have required confirmation by actual printing trials whenever new variables were introduced. Examples of this "quick and easy" type of test are the wet thumb test (10,11), the dry rub test (10), the sealing wax test (11), the Dennison (12,13) and K and N (13) wax tests, and the "Scotch" or friction tape test (14). The resistance-to-picking tester of Bekk (15) may be considered a refined and modified version of the sealing wax test.

It is concluded that no single test, or type of test, has met with complete and universal acceptance as a means of evaluating the pick strength of coated papers. Ignorance of the exact nature of the stresses applied during printing seems to be a major source of difficulty. Different tests apply different stress situations; and little effort is made to impart simple, uniform, and reproducible stress configurations to the specimen. In the IPC bonding strength tester, for example, the stresses (shown qualitatively in Appendix A) are so complex and overlapping that the particular stress causing failure is open to question and, indeed, may vary from one coated specimen to another. For most coating strength tests the criterion seems to be (and rightly so in the immediate practical sense): "Do the test results correlate with the performance of the paper in the printing press?"

Just as the path to greater understanding in other areas has often been to study a complex operation in simplified form and sometimes by

parts or components, it is suggested that a more fundamental understanding of coating strength may be achieved by examining simplified systems subjected to precisely defined stress situations. The results of such limited studies must, of course, be carefully interpreted in the light of their restricted stress situations.

As a step in the direction of more fundamental coating strength investigation, it is proposed to study the behavior of a simple clay-starch coating under the influence of a uniform tensile stress applied perpendicularly to the plane of the coating. This strength property, called transverse tensile strength (TTS), is defined as that tensile stress required to cause failure in a sheetlike specimen when a uniformly distributed stress is applied perpendicularly to the plane of the specimen. TTS has been selected because it appears to play a very significant, if not dominating, role in pick strength. Attempts to equate TTS with pick strength have been unsuccessful. The staff of The Institute of Paper Chemistry (16) tried to correlate the picking force, measured as a transverse tensile strength, with the critical Dennison wax number for casein-clay coatings. Even though the critical wax number correlated fairly well with the casein content, they could find no correlation between picking force and the critical wax number or casein content.

It is apparent that TTS and pick strength cannot be completely synonymous because other types of stress, such as shear and bending, may be involved in pick strength; however, this fact does not nullify the possible contribution of TTS to pick strength. It merely emphasizes the point that other stress components must also be considered in the eventual elucidation of pick strength.

With the stress configuration delimited to that described above as a transverse tensile stress, it is desired to impose the additional restriction that failure must occur within the coating. The substrate is thus to be considered only in terms of its contribution to the final properties of the coating, for example, by its effect on the loss of vehicle from the coating by penetration into the substrate. There are two reasons for this restriction: (1) Failure of coated paper under printing conditions usually occurs within the coating. (2) Failure under pure transverse tensile stress might occur in the substrate, but such a failure would be of minor significance to a quantitative understanding of coating strength.

As a consequence of this restriction, the substrate, if weaker than the coating, must be either strengthened or removed from the coating, or else the coating must be weakened below the strength of the substrate.

THE TRANSVERSE TENSILE STRENGTH (TTS) OF PIGMENT COATINGS

Considering the coated substrate as a multilayer system, as depicted in cross section in Figure 1, there are three major components in the TTS of the system:

1. Cohesive strength of the substrate
2. Adhesive strength of the substrate-coating bond
3. Cohesive strength of the coating

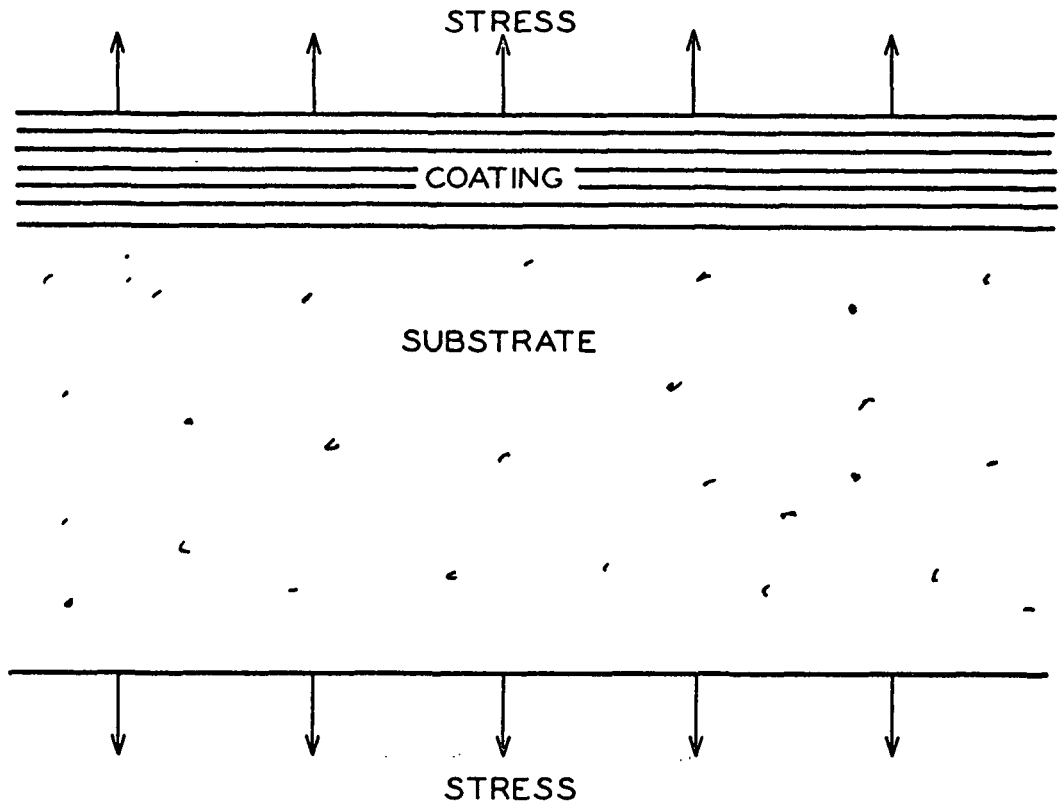

Figure 1. Substrate-Coating System

It is assumed that the strength of the substrate and the interfacial bond are sufficient for failure to occur within the coating.

The cohesive strength of the coating is modified or determined by three groups of variables:

1. Primary variables acting uniformly throughout the coating

2. Primary variables tending to differentiate "layers" within the coating

3. Secondary or process variables affecting strength indirectly through one or more primary variables.

These variables will be discussed under the above groupings. Since the TTS of the coating will be limited by its weakest layer, the following variables are evaluated in terms of their probable contributions to the formation of weak layers within the coating.

GENERAL COATING STRENGTH VARIABLES

The following variables are believed to affect TTS nearly uniformly throughout the coating and probably have a minor effect in producing layers of different strengths within the coating.

THE COHESIVE STRENGTH OF THE ADHESIVE

The cohesive strength of the coating adhesive is a function of its molecular composition and structure. In pigment coatings the adhesives usually bond through the interaction of secondary valence forces (Van der Waal's forces). Of these, the electrostatic forces of strongly polar groups undoubtedly account for the strength of such adhesives as starch, casein, gelatin, and soya protein. The chain length, the chain-length distribution, and the number and the configurations of branch chains of the adhesive molecules are important factors in secondary valence bonding. The longer chain lengths contribute increased tensile strength in the direction of their orientation by supplementing the weaker secondary valence linkages with primary chemical bonds. The orientation of adhesive molecules will thus modify the contribution of longer chains to

strength in a given direction. The branch chains offer more possibilities for molecular interaction but less opportunity for molecules to align with each other over large portions of their length.

Although vehicle movement through the coating may cause the concentration of shorter adhesive molecules in some zones, the quantitative aspect of adhesive concentration is probably of more significance than the chain-length distribution within the coating.

The nature of the bonding forces between adhesive molecules and the molecular orientation of the adhesive appear to be of minor importance in promoting different layer tensile strengths.

THE COHESIVE STRENGTH OF THE PIGMENT

The cohesive strength of the clay platelets is determined largely by hydrogen bonds between the kaolin crystal planes. Strong primary valence forces provide lateral strength in the platelets. The orientation and density of secondary valence bonding between platelets in an intact clay particle is likely to exceed that of the amorphous adhesive. If the pigment particles are so poorly dispersed that they do not act individually, the cohesive strength of loose aggregates could become the critical strength factor. For well-dispersed coatings the pigment strength should be sufficient to prevent failure within the clay particles.

THE ADHESIVE STRENGTH OF THE PIGMENT-ADHESIVE BOND

The two adhesives most widely used in pigment coating, starch and casein, have polar groups on their molecules. The clay platelets likewise present areas of strong electrostatic force on their surfaces.

As the pigment particles are reduced in size by grinding or other treatment, the surface forces become more influential; and bonding to polar adhesives is facilitated.

The sites of polar force on the clay surfaces are subject to contamination by foreign ions or molecules or may be partially masked by a layer, or layers, of adsorbed water or other polar solvent. The increased effectiveness of adhesives that are brought into intimate contact with the clay pigment under conditions of high shear may be due to the more effective adsorption of adhesive molecules on the fresh pigment surfaces generated by the shearing action.

Although the adhesive-pigment bond is potentially very strong, the interference of other substances, such as solvent molecules or contaminating ions, may reduce the effectiveness of the bond but is unlikely to cause systematic variation within the coating.

THE DIFFERENCE IN ELASTIC MODULI OF THE ADHESIVE AND PIGMENT

If the moduli of elasticity of the pigment and the adhesive were equal, the stresses in a coating free of voids, inclusions, or other stress raisers would tend to be uniformly distributed. When a large difference exists between the moduli of elasticity of the adhesive and the pigment and the load is carried partly by each, the stress distribution is almost certain to be highly irregular. The extent of the difference in moduli and the detailed geometry of the system are unknown.

In general, pigment coatings, and layers within coatings, are handicapped strengthwise by differences in elastic moduli of pigment and adhesive.

LAYER COATING STRENGTH VARIABLES

The following variables may contribute to different layer transverse tensile strengths by being functions of transverse position within the coating. Variables that show a systematic variation with transverse position are of particular interest to those concerned with efficient adhesive utilization, even though such variables are not yet subject to rigorous evaluation.

VOID VOLUME DISTRIBUTION

The void volume within the coating affects strength because the cross-sectional area bearing the tensile load is thereby reduced. A non-uniform distribution of voids in the coating will have a significant effect on strength. A zone of weakness is created when a layer of greater void volume than adjacent layers is formed. Movement of vehicle and/or adhesive either toward the surface or toward the substrate is likely to cause stratification in the pigment packing and distribution of voids. Although Kraske (17) has characterized the pore size distributions of several coatings as a whole, accurate information on the location of voids within pigment coatings is not available.

STRESS CONCENTRATION DISTRIBUTION

A by-product of increased void volume in a coating is a concentration of the total stress over a smaller cross-sectional area of solids. Because of the exceedingly complex structure of pigment coatings it is virtually impossible to accurately describe or analyze the stress conditions that occur within the coating. It can be concluded, however,

that any factors tending to increase stress concentration will adversely affect the strength of the coating. Voids, highly irregular pigment particle shapes, foreign inclusions, differences in particle orientation, and minute cracks or defects in the coating are all potential stress raisers and can thus reduce the strength of the coating. Stress concentrations are likely to vary in number and magnitude throughout the coating, but measurement of this variation is not yet possible.

RESIDUAL STRESS DISTRIBUTION

Solvent removal, different coefficients of thermal expansion between pigment and adhesive, and different hygroexpansivities of the coating components are factors capable of producing residual stresses leading to uneven stress distribution, i.e., stress concentrations. The strength of the coating is correspondingly reduced.

Because of the planar shape of the coating the air surface and the substrate-coating interface are more vulnerable to drying, heating, cooling, and humidifying treatments than is the interior of the coating. This situation may result in strength differentiation between coating "layers". When the surface layer dries first, for example, the subsequent drying and dimensional changes of the underneath layers will tend to set up residual stresses in the coating.

PARTICLE ORIENTATION

For nonspherical pigment particles, orientation is a factor in determining the strength of the coating. Clay particles shaped like platelets are particularly susceptible to orientation. This fact is used in the preparation of oriented-aggregate specimens for the x-ray

diffraction analysis of clay minerals. Centrifugation may be used to facilitate orientation, or the clay may be merely deposited from a water suspension by drying.

The effect of orientation on strength can be visualized by imagining first an intact brick wall and secondly the bricks arranged randomly in a pile with the same mortar-to-brick ratio as in the wall. If the mortar were free to flow when the brick pile was formed, an initially uniform mortar distribution would soon lose its uniformity as the mortar collected at the lower levels, depriving the upper bricks of part of their mortar. The analogy with a clay coating is that when clay particles are randomly oriented there is probably a nonuniform void distribution and an associated nonuniform adhesive distribution.

If the clay particles next to the substrate are better aligned so that a more uniform, void-free coating layer is formed, the TTS should be greater near the substrate than near the air surface of the coating if it is assumed that both pigment and adhesive contribute to strength in direct proportion to their volumetric concentrations. Failure in TTS would then occur in the weaker layers near the air surface.

On the other hand, if the adhesive is the principal means of resisting tensile stresses, i.e., the pigment does not share the load in proportion to its volumetric concentration, a layer of increased particle alignment could be a layer of weakness because of a lower volumetric concentration of adhesive due to squeeze-out or migration.

ADHESIVE DISTRIBUTION

The adhesive ratio (parts adhesive/100 parts pigment) is a major variable in producing pigment coatings of a given strength. Higher contents of adhesive may increase strength by forming more adhesive-pigment bonds, reducing the void volume, relaxing stresses, decreasing stress concentrations, and increasing the cohesive strength of the adhesive.

The effect of the initial adhesive ratio on the "wax pick" strength of pigment coatings is shown in Figures 2 and 3 for several adhesives and pigments. The strong dependence of "wax pick" strength on adhesive content is clearly shown. It seems probable that TTS is likewise dependent on the initial adhesive ratio.

It is worth noting that the final adhesive ratio in the dried coating not only can differ from the formula ratio but also can vary from region to region within the coating. Such variations in adhesive content are more the rule than the exception in commercial pigment coatings.

Changes in the adhesive ratio with increasing distance from the surface of the coating result in regions or layers of unequal TTS. Singleterry (20) has observed that the zone of failure in casein-clay coatings of low initial adhesive ratio occurs in the coating about a micron away from the bodystock-coating interface. He postulated a zone of lower adhesive content to explain this phenomenon.

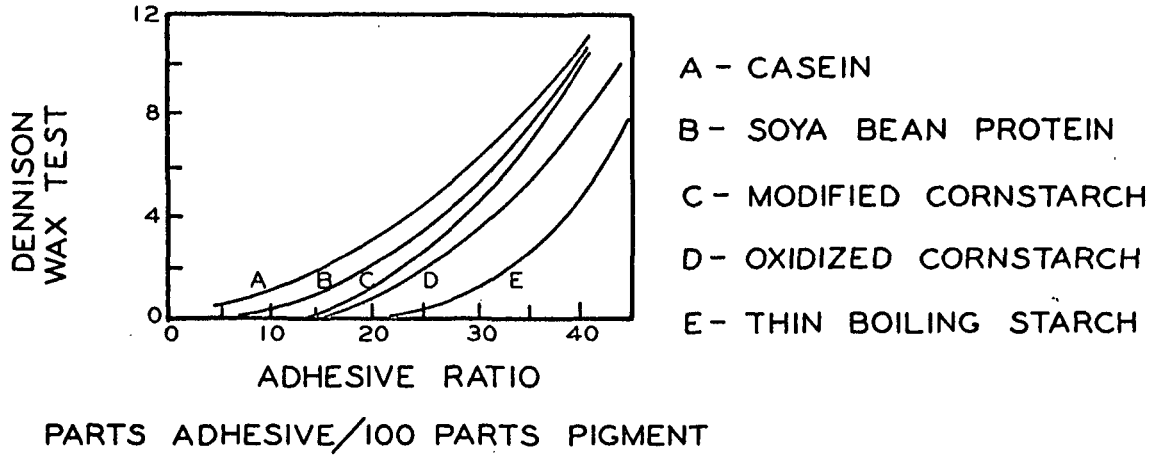

Figure 2. Pick Strength vs. Adhesive Ratio for Calcium Carbonate and Various Adhesives (18)

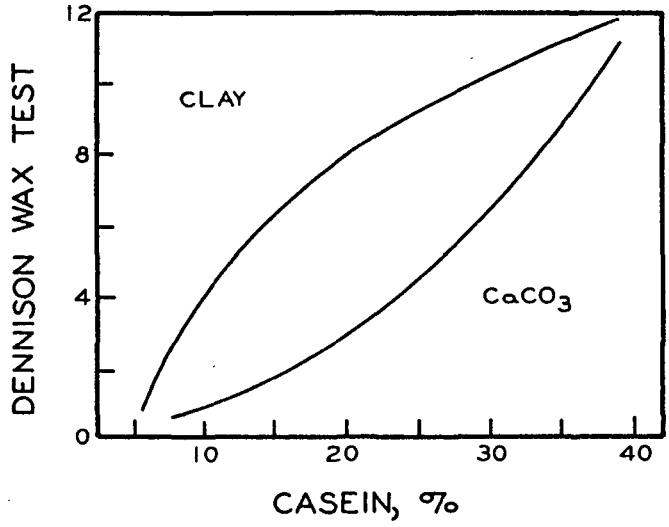

Figure 3. Pick Strength vs. Percent Casein for Clay and Calcium Carbonate (19)

The migration of starch in clay coatings by (1) penetration into the bodystock and (2) movement with the vehicle during drying was studied by Dappen (21). Limitations in the techniques of analysis made it difficult to draw rigorous conclusions about adhesive distributions in coatings of commercial weight (15 to 25 lb./ream--25x40-500) on glass or near the bodystock interface in coatings on paper. Air-dried coatings seemed to have a uniform adhesive distribution, whereas hot-air, blast-dried coatings had a pronounced adhesive concentration near the surface exposed to the air (Figure 4).

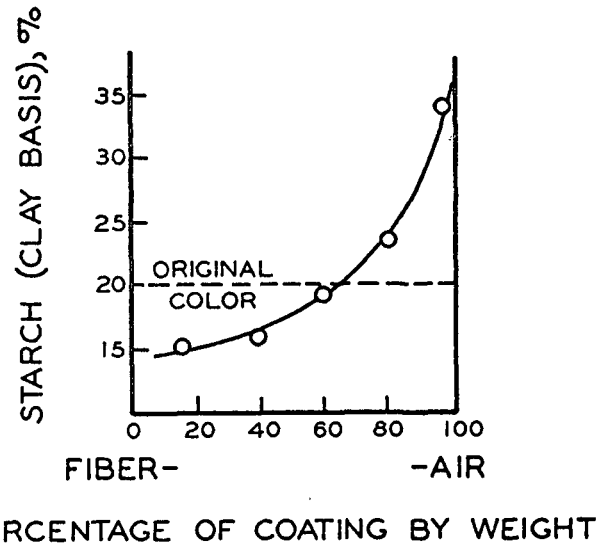

Figure 4. Distribution of Starch in Coated Paper Dried with a Hot Air Blast (21)

The adhesive distribution in the coating near the bodystock interface has not been characterized. Nor have the adhesive distributions in coatings of commercial weight or thickness (15 microns) been adequately measured.

PROCESS VARIABLES

Variables encountered in the preparation of pigment-coated paper that can affect the TTS of the coating are considered in this section.

COATING FORMULATION

The kind and amount of substances included and the manner of treatment to produce a satisfactory coating color are of first importance in establishing the strength potential of the coating. The pigment, adhesive, and dispersing agent are essential components. Ways in which the pigment and adhesive affect strength have been discussed above. The adhesive ratio has been emphasized as an important variable. The effect of the dispersing agent on coating strength is unknown; but it probably acts indirectly through other factors such as the adhesive-to-pigment bond strength.

The method of preparing the coating influences its strength. Mixing the adhesive and pigment at high solids (65-75%) and diluting to 50% can produce stronger coatings than simply mixing at 50% solids. The reasons for this strength improvement may include improved adhesive-to-pigment adhesion, better adhesive retention within the coating, and/or a more uniform adhesive distribution.

SOLIDS CONTENT

The per cent solids of the coating as it is applied to the bodystock affects the final strength of the coating. High solids (55%) coatings need less adhesive than do low solids (40%) coatings for the same final

transverse tensile strength. Part of the strength increase may be due to the high solids mixing advantages cited above, but it is quite probable that an additional improvement stems from reduced adhesive migration.

METHODS OF APPLYING COATING

Because of the large difference in density between the pigment and the coating vehicle, the possibility of pigment sedimentation under the centrifugal force of high-speed roll coating was checked by calculation (Appendix A). Assuming a peripheral speed of 1800 feet/min. and a roll diameter of one foot and applying Stokes's law, the displacement in one half turn of the roll for 1.0 micron (equivalent spherical diameter) clay particles suspended in water is about 0.4 micron. In a commercial coating the vehicle viscosity is several times that of water, and particle interaction could be significant. It is concluded that particle displacement due to high-speed roll coating is inconsequential in present-day commercial coating practice.

Particle orientation may be affected by the methods of applying, distributing, and smoothing the coating; but no evidence is presently available. A systematic variation in particle orientation between body-stock and surface would tend to cause a gradation in the "layer" strength of the coating. The finer capillary structure of better particle orientation is thought to be capable of greater retaining affinity for the liquid vehicle with its adhesive.

SUBSTRATE

The substrate to which the coating is applied affects the internal TTS of the coating through three factors:

1. Surface geometry
2. Porosity
3. Receptivity for the coating components

The surface geometry on the scale of the pigment particles affects TTS by influencing particle orientation at the interface. A more planar substrate, through better particle alignment, could reduce stress concentration, adhesive concentration, voids, and residual stresses. Mechanical bonding at the interface, however, is facilitated by surface fissures and reentrant angles.

The substrate porosity and receptivity control the absolute and the relative quantities of the coating components that are separated from the surface coating and can no longer contribute to its internal strength. Porosity refers to the structural aspect of opening sizes, whereas receptivity includes wettability, electrostatic, and electrokinetic effects. Porosity permits a mechanical filtering of particles above a certain size, and pore plugging is a possible consequence of this action. The receptivity of the substrate primarily affects the rate of penetration. Factors influencing penetration rate, other than pore size and receptivity, are the viscosity of the penetrating phase and the forces in the coating tending to resist the separation of the penetrating phase from the coating.

Vehicle penetration, with or without adhesive, into the substrate is likely to alter the adhesive distribution within the coating, particularly if there is little selective adsorption of the adhesive on the pigment. It is generally believed that a certain amount of adhesive penetration is desirable to secure good bonding of the coating to the bodystock. Since coatings on aluminum foil exhibit excellent bonding without penetration, possibly the observed beneficial effect of adhesive penetration into fibrous bodystock is the result of better bonding of surface fibers, some of which may have been loosened by the coating solvent.

DRYING

The removal of solvent from the coating usually entails the movement of liquid from the interior of the coating toward the surface and subsequent evaporation of the liquid. The mechanism of the hot surface drying of paper has been investigated recently by Dreshfield and Han (22) who confirmed that liquid water migrated from the inner regions toward the surface zones of evaporation. Adhesive migration in drying pigment coatings is evidenced by the work of Dappen (21) with clay-starch coatings on glass. In coatings dried by a hot-air blast he found higher adhesive contents in the surface layers of the coating than in the layers underneath. Air-dried coatings on glass showed a more uniform adhesive distribution.

The method and rate of drying are therefore of significance to the TTS of layers within the coating. Any drying technique involving liquid migration in the coating will tend to change the adhesive distribution.

In addition, drying can reduce strength by the creation of residual stresses when one layer dries before another with accompanying dimensional changes.

PRESENTATION OF THE PROBLEM

As a step toward a more fundamental understanding of the pick strength of pigment-coated paper, it is proposed to evaluate the role of adhesive distribution in determining the internal TTS of clay-starch coatings.

Void volume distribution, stress concentrations, residual stresses, and particle alignment are believed to affect TTS; but their relative contributions to TTS are thought to be subordinate to, or dependent on, the adhesive distribution.

The coating to be studied has the following components:

1. Secondary Georgia kaolin with a narrow particle size range
2. Hypochlorite-oxidized cornstarch of low viscosity
3. Sodium hydroxide for pH adjustment
4. Quadrafos, $Na_6P_4O_{13}$, for dispersing the kaolin
5. Water

The TTS of the substrate is not a factor in this study since failure will be constrained to the coating.

The two major objectives are: (1) to develop a means of measuring the internal TTS of clay-starch coatings; (2) to analyze the TTS behavior of clay-starch coatings as a possible function of adhesive distribution.

The experimental approach selected is (1) to vary certain factors known or believed to affect adhesive distribution, and then (2) to determine the TTS, the location of failure, and the net adhesive ratio

of the coating. The independent variables chosen for this study are:

1. Pigment particle size
2. Substrate pore size
3. Initial adhesive ratio
4. Method of drying
5. Coat weight.

GLOSSARY

TTS -- transverse tensile strength, defined as the tensile stress required to cause failure in a sheetlike specimen when the tensile stress is uniformly distributed and perpendicular to the plane of the specimen.

"MF" -- Millipore Filter, made by Millipore Filter Corporation.

Meaning of coating symbols, e.g., 12MV -- the first two digits represent the initial adhesive ratio of the coating; the first letter stands for the clay fraction used in the coating (S = 0.0 - 0.5 mu., M = 0.5 - 1.0 mu., L = 1.0 - 2.0 mu.); the second letter identifies the substance to which the coating was applied (V = "MF", type VC; H = "MF", type HA; A = "MF", type AA; F = aluminum foil; K = Kodapak); and the subscript HAB means the coating was dried with a hot air blast.

Adhesive ratio -- parts starch/100 parts pigment, by weight

Net adhesive ratio -- adhesive ratio of the coating layer after drying and is less than the initial, or formula, adhesive ratio if adhesive has penetrated into the substrate.

VVP -- viscosity-velocity product, a measure of the stress causing failure in the IPC bonding strength tester or the IGT printability tester; the viscosity is that of the test film whose splitting exerts tensile stresses on the specimen, and the velocity refers to the peripheral speed of the wheel carrying the specimen, at the instant of failure.

Apparent density -- weight of coating/total volume of coating; total volume includes the volume of pores within the coating.

lb./ream -- coating weight is expressed as lb. coating/ream for a ream size of 25 x 38 in.--500 sheets, representing an area of 475,000 $in.^2$ or about 3300 $ft.^2$

e.s.d. -- equivalent spherical diameter, an expression of particle size as the diameter of a sphere which falls at the same rate as the particle in a viscous medium.

σ_i -- standard deviation of the individual, the root mean square of the deviations from the mean.

σ_m -- standard deviation of the mean, the standard deviation of the individual divided by the square root of the number of individuals on which the mean is based.

THE SYSTEM: DESCRIPTION OF MATERIALS

THE OVER-ALL SYSTEM

The system under consideration is a pigment coating consisting of clay, starch, sodium hydroxide, Quadrafos (sodium tetraphosphate--$Na_6P_4O_{13}$, made by Rumford Chemical Works), and water.

Affecting the system, but not a direct part of it, is the substrate to which the coating is applied. Three classes of substrates were used:

1. Kodapak--a nonporous sheet of cellulose acetate butyrate made by Tennessee Eastman Corp. and soluble in certain organic solvents such as ethyl acetate and acetone
2. Aluminum foil--0.006 inches thick
3. Millipore Filter ("MF")--a synthetic, porous sheet material made by Millipore Filter Corp. and soluble in organic solvents such as ethyl acetate and acetone.

In addition to the reasons given later, the choice of clays and starch was influenced by the fact that related studies on the physical structure of pigment coatings were being carried out by D. J. Kraske (17). By the choice of similar materials the results of the two investigations could be combined to provide an understanding of coating behavior that would not be possible if different pigments and adhesives were used.

CLAYS

The three particle size fractions of "Lustra" coating clay were obtained by D. J. Kraske from Southern Clays Inc. Kraske (17) has described the clays in detail, but the information pertinent to this study is included below for completeness.

Prior to fractionation the clay had been dispersed with tetrasodium pyrophosphate. After fractionation the clay was flocculated with sulfuric acid and then oven dried.

Particle size distributions obtained by the centrifuge method and expressed in terms of equivalent spherical diameter (e.s.d.) are shown in Figure 5 (17). The three clay fractions are identified by the nominal particle size range or the code letters given in Figure 5.

The surface areas and length-to-thickness ratios determined by Kraske (17) are given in Table I.

TABLE I

PHYSICAL CHARACTERISTICS: CLAY FRACTIONS (17)

Coating Code Letter	Nominal Particle Size, microns	B.E.T., [a] Surface Area $m.^2/g.$	Length/Thickness Ratio
S	0.0-0.5	20.15	6.0
M	0.5-1.0	14.04	7.7
L	1.0-2.0	10.30	10.0

[a] Brunauer, Emmett, and Teller method

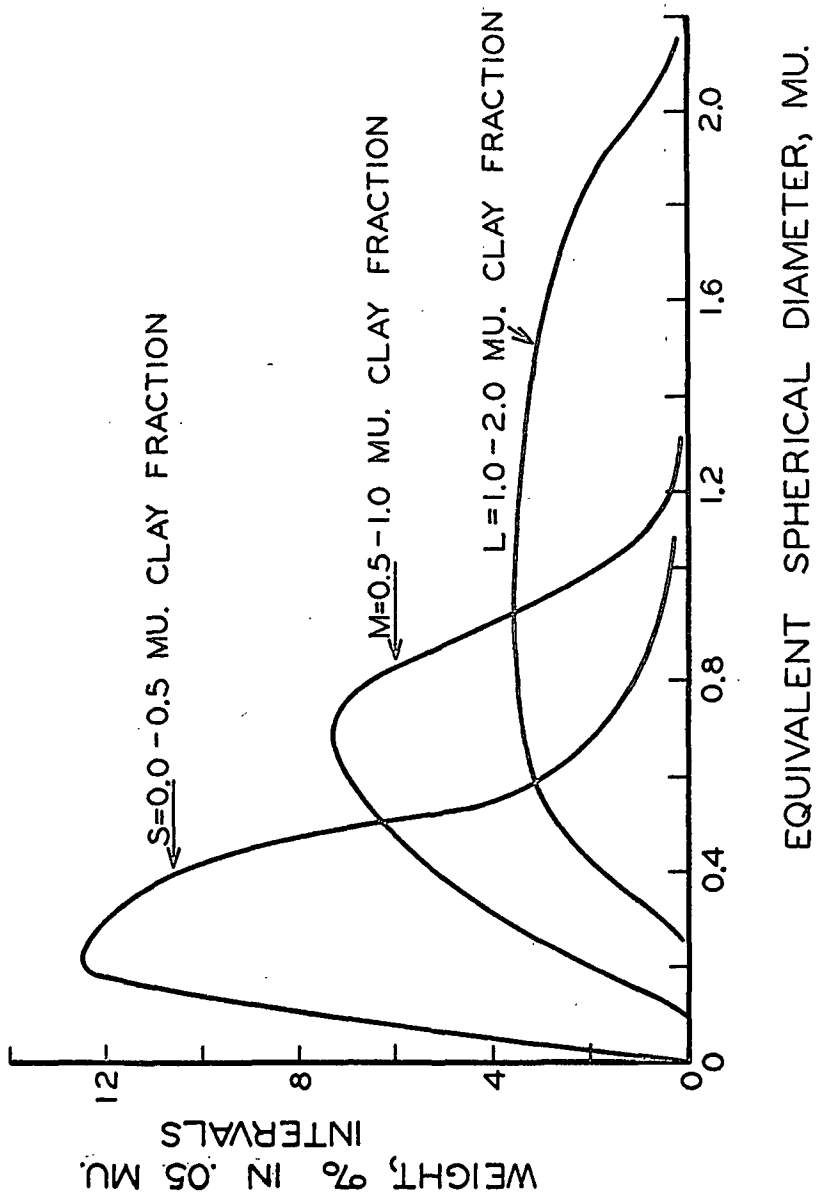

Figure 5. Particle Size Distributions (17)

From electron micrographs and x-ray examination Kraske (17) found no evidence of nonkaolin impurities, even in the smallest fraction, which had less well-defined hexagonal platelets. He determined the dispersing agent requirement for minimum viscosity as 2 to 3 milli-equivalents of Quadrafos for 100 grams of clay, after adjusting the clay slip to pH 8.0 with 1.0N sodium hydroxide.

STARCH

Because of its widespread use in the pigment coating of printing papers and its availability in sufficient quantity with uniform properties, a modified starch was chosen. The particular product used was Stayco M, a hypochlorite-oxidized cornstarch supplied by A. E. Staley Co.

The starch was slurried at 25% solids in distilled water and cooked in the Corn Industries viscometer, described by Kesler and Bechtel (23), at 96°C. for 30 min. After cooking, the starch was cooled to 50°C. and held at this temperature until it was added to the clay slip. In no case was the starch preparation held at 50°C. longer than three hours.

Characteristic values obtained during the starch cook are as follows:

Temperature at start of swelling = 62°C.
Maximum torque during the cook = 260 g. cm.
Temperature at maximum torque = 69°C.
Torque at 50°C., after cooking = 12 g. cm.

SUBSTRATES

The Kodapak and the aluminum foil have been sufficiently described above, but more information about "MF" is needed for an adequate appreciation of its properties.

1. Smoothness

The surface of "MF" is very smooth, similar to that of cast-coated papers such as Kromekote. The smoothness increases with decreasing pore size for the three types used in this study.

2. Pore characteristics (24)

The pores in "MF" are unusual in two ways: (1) They are perpendicular to the filter surface and thus provide essentially direct passages through the filter. (2) They have a narrow and well-defined size range from each type, as shown in Table II.

TABLE II

PORE SIZE CHARACTERISTICS OF MILLIPORE FILTER (24)

Coating Code Letter	Millipore Filter Type	Pore size, mu	Pore Diameter Variations, mu	Rates of Flow, cc./cm.^{2}/min. at 25°C. and 70 cm. Hg	
				Water	Air
V	VC	0.100	0.008	3.6	600
H	HA	0.45	0.02	72	9,600
A	AA	0.80	0.05	330	33,000

The pore volume of "MF" is given as 80% of the total volume of the sheet.

3. Solubility and chemical resistance

"MF" is not affected by water or dilute alkalies but is soluble in acetone, ethyl acetate, and certain other organic solvents.

4. Refractive index

"MF" becomes transparent when impregnated with oil of refractive index 1.50.

5. Thickness variations

Although "MF" is very smooth, it does show significant changes in thickness over a span of several inches. This thickness variation must be corrected if coatings of uniform thickness are to be applied by a drawdown technique.

EXPERIMENTAL METHODS

PREPARATION OF COATINGS

FORMULATION

A typical coating formula is as follows:

Weight of Solids, g.	Component		Total Weight, g.
200	Clay, 1.0-2.0 mm at 99.4% solids	=	201
24	Starch at 25% solids	=	96
	NaOH, 1.0N	=	9
	Quadrafos ($Na_6P_4O_{13}$), 1.0N	=	6
	Water	=	95
224	at 55.0% solids	=	407

The clay is added to the solution of sodium hydroxide and Quadrafos in distilled water under agitation with a Hamilton Beach stirrer. About 10% of the sodium hydroxide and water called for in the formula is withheld for later adjustment of the pH and solids content of the coating. When the clay slip has been stirred for at least 30 min. or until the clay is well dispersed, the required amount of starch is weighed into the clay slip. The starch preparation has been described in the above section on materials.

After the coating is thoroughly mixed, the pH is adjusted to 8.0 with 1.0N NaOH. The coating is then passed twice through a hand-operated dispersion mill (Chicago Apparatus Co., no. 22950) and once

through a 325-mesh screen. The solids content of the coating is determined and then adjusted to 55.0% by adding water.

According to Kraske (17), Hercules Viscometer rheograms of coatings prepared as above show that these coatings are pseudoplastic with a relatively low viscosity, less than one poise. The fine particle size clay fraction had a yield value of about 60,000 dyne cm.

APPLICATION

The coating color was applied to the various substrates with a 1.5-mil Bird applicator bar. On the nonporous substrates, Kodapak and aluminum foil, the drawdowns were made on samples 6 x 8 in. in size and the built-in clearance of the Bird bar dictated the coat weight. On the porous "MF" substrates, since better coat weight control was desired, either the 4 x 5 in. sheets of "MF" or the zones where the supporting surfaces of the Bird bar travelled were shimmed with thin strips of metal stock. In some cases, shims were used both under the "MF" and under the Bird bar.

The variations in thickness across 4 x 5 in. handsheets mentioned in the description of materials required a further step to improve the uniformity of coat weight. Guard strips about 1/2-in. wide were cut from the sides of each "MF" handsheet and attached over the edge shims with tape so that the Bird bar rested directly on the guard strips during the drawdown. In this way thickness variations within the handsheets had less influence on the coat weight.

ISOLATION

In preliminary experimental work it became apparent that the coating was considerably stronger in TTS than was the "MF" for adhesive ratios in the range of interest (above 10). To determine the internal TTS of the coatings on "MF" it was therefore necessary to remove the substrate.

The coatings on "MF", after drying at 73°F. and 50% R.H. (unless otherwise specified), were isolated from "MF" by the ethyl acetate treatment developed by Kraske (17). The handsheets were cut into four smaller rectangles and passed through seven baths of ethyl acetate, 10 min. in each bath. In the fifth bath the coatings, which were supported on wire screens with the substrate side up, were gently brushed with small camels' hair brushes to remove the portion of the coating that had penetrated the substrate and was only very weakly held to the coating. Sometimes the starch that had penetrated the coating was observed to float away from the coating as a film. Thus, a qualitative estimate of the nature and extent of penetration losses could be made.

After the isolated coating is removed from ethyl acetate and dried, it is stored in humidistats at a known relative humidity (52% R.H. in most cases).

Kraske (17) concluded that the ethyl acetate isolation method "accomplishes essentially complete solution of the raw stock without detectable effects upon the strength, the clay particle orientation, the surface area, and the pore distribution of coatings."

Coatings isolated with ethyl acetate and conditioned at 52% R.H. lost from 0.5 to 1.6% of their initial weight on oven drying at 105°C. In addition, Kraske (17) found that from 0.03 to 0.20% of the initial weight is lost from the oven-dried coating if the coating is soaked in water and then oven dried again. He attributed this to the release of solvent previously trapped in the coating.

DETERMINATION OF TRANSVERSE TENSILE STRENGTH

BACKGROUND

Several bonding strength tests have been cited in the introductory section, ranging from "quick and easy" methods to press simulation tests; but none of these tests imparts a simple, uniform transverse tensile stress to the specimen. Recognition of the importance of TTS is not new, however, for a method to measure the TTS of paper was described as early as 1923. In this method by an anonymous author (25) a paper sample is bonded between wood test blocks with sealing wax and then pulled apart in a Schopper tensile tester. TTS values between 60 and 100 lb./in.^{2} were obtained for a range of papers. The principle of this method had been applied earlier to evaluate the adhesive strength of glues.

In 1925, Abrams (26) modified the test by using silicate and cellulosic adhesives. Kessler (27) devised metal adapters to replace the wooden blocks. Sutermeister and Porter (28) used brass blocks, sodium silicate adhesive, and a Schopper tensile tester. Brecht and Blikstad (29) using wood cylinders reported strengths ranging from

about 30 lb./in.^{2} for blotting paper to about 340 lb./in.^{2} for glassine. Sutermeister and Osgood (30) avoided the interference of adhesive penetration by using tacky sheet rubber such as is used for tire repairs. They applied air pressure to a piston linked to the test block to cause rupture. The staff of The Institute of Paper Chemistry (16) experimented with brass plates and shellac, and later with Dennison waxes as the adhesive.

In nearly all cases where coated papers were tested by the "block TTS test", in any of its above variations, the failure was found to occur in the substrate, not the coating. Perhaps this fact has discouraged further development and use of this type of test for coated papers. As noted earlier, much emphasis has been placed on tests that simulate end-use conditions. Nevertheless, there have been other serious objections to the "block TTS test". The staff of The Institute of Paper Chemistry (31) emphasize the importance of applying a normal tensile stress to the specimen by a means which does not (1) appreciably change the temperature of the specimen, (2) alter the moisture content of the specimen, or (3) cause the adhesive to penetrate appreciably into the specimen. They also cite the possible interference of stress intensification due to edge effects and nonuniform thickness of sample.

With the above historical information as background the prerequisites of a satisfactory TTS test for pigment coatings can be more precisely described.

PREREQUISITES OF TTS TEST

Adhesive

An adhesive ideally suited to the measurement of the TTS of clay-starch coatings must:

1. Bond clay-starch coatings to steel with at least 3000 lb./in.^{2} tensile strength.
2. Be capable of application as a uniform layer.
3. Bond to porous coatings with negligible penetration (less than one micron).
4. Require neither temperatures above 80°C. nor pressures above 100 lb./in.^{2} for bonding.
5. Not require release of solvent after bonding is initiated.
6. Not set up stresses during processing.
7. Be capable of use in a vacuum to avoid the entrapment of air in the joint.

Mounting Samples

The requirements of an apparatus for mounting samples for the evaluation of TTS are:

1. Maintain precise alignment of mating test cylinders on a common axis.
2. Provide a means of doctoring a uniform layer of adhesive on the ends of the test cylinders.
3. Support test specimens between test cylinders, without contacting either cylinder prior to clamping.
4. Clamp specimens at any desired pressure between 0 and 100 lb./in.^{2}.
5. Clamp twelve or more specimens simultaneously.
6. Fulfill the above requirements while sealed inside a vacuum.
7. Disassemble for easy removal of test cylinders.

Testing Samples

After the specimen is bonded to mating test cylinders, it must be stressed by an arrangement that will:

1. Positively align the axis of the test cylinders with the direction of the applied stress so that a uniform transverse tensile stress is exerted on the specimen.
2. Support a load of at least 1000 lb.
3. Provide an easy and rapid means of attaching and detaching the test cylinders.

SOLUTION TO ABOVE PREREQUISITES

Adhesive

An adhesive consisting of an epoxy-type resin with an inorganic filler and an amine catalyst was found to satisfy the above requirements for an ideal adhesive. The resin and catalyst are manufactured and sold by Armstrong Products Co. under the names Armstrong Adhesive A-1 and Activator A.

When the catalyst and resin are first mixed, the adhesive is quite workable and may be doctored onto a surface using a suitable scraper. At this stage the adhesive tends to level itself. About 20 min. after the catalyst and resin are mixed, the adhesive becomes very stiff and starts to gel. The extent of penetration of adhesive into the sample may be controlled by the time allowed for the adhesive to cure before the bond is formed. The clamping pressure also affects adhesive penetration into the sample.

Mounting Samples

An apparatus for mounting samples for the evaluation of TTS was designed and built to fulfill the requirements listed above. Figures 6 through 9 show various aspects of the apparatus.

In Figure 6 the components of the apparatus are identified as follows:

A--Lower half of apparatus.

B--Plate for supporting specimens before they are clamped.

C--Upper half of apparatus.

D--Test cylinders (24 required), 1/2-in. diameter x 1-in. long, one end smooth and the other center-drilled and tapped to receive a 1/4-in.--28NF thread; both ends are accurately faced perpendicular to the axis of the cylinder.

E--Cap screws (12 required) for retaining the test cylinders in the upper half of the apparatus before the specimens are clamped.

F--Yoke for turning nut (G) by means of a rod with a wedge-shaped tip which engages the slot in the yoke.

G--Nut to compress spring.

H--Spring and collar.

J--"T" crank, used with ejector.

K--Ejector to remove test cylinders from lower half of apparatus, after the specimens have been mounted, without stressing the specimens.

In Figure 7 the test cylinders are in the apparatus, and the samples are in position on the plate. The apparatus is now ready for the adhesive

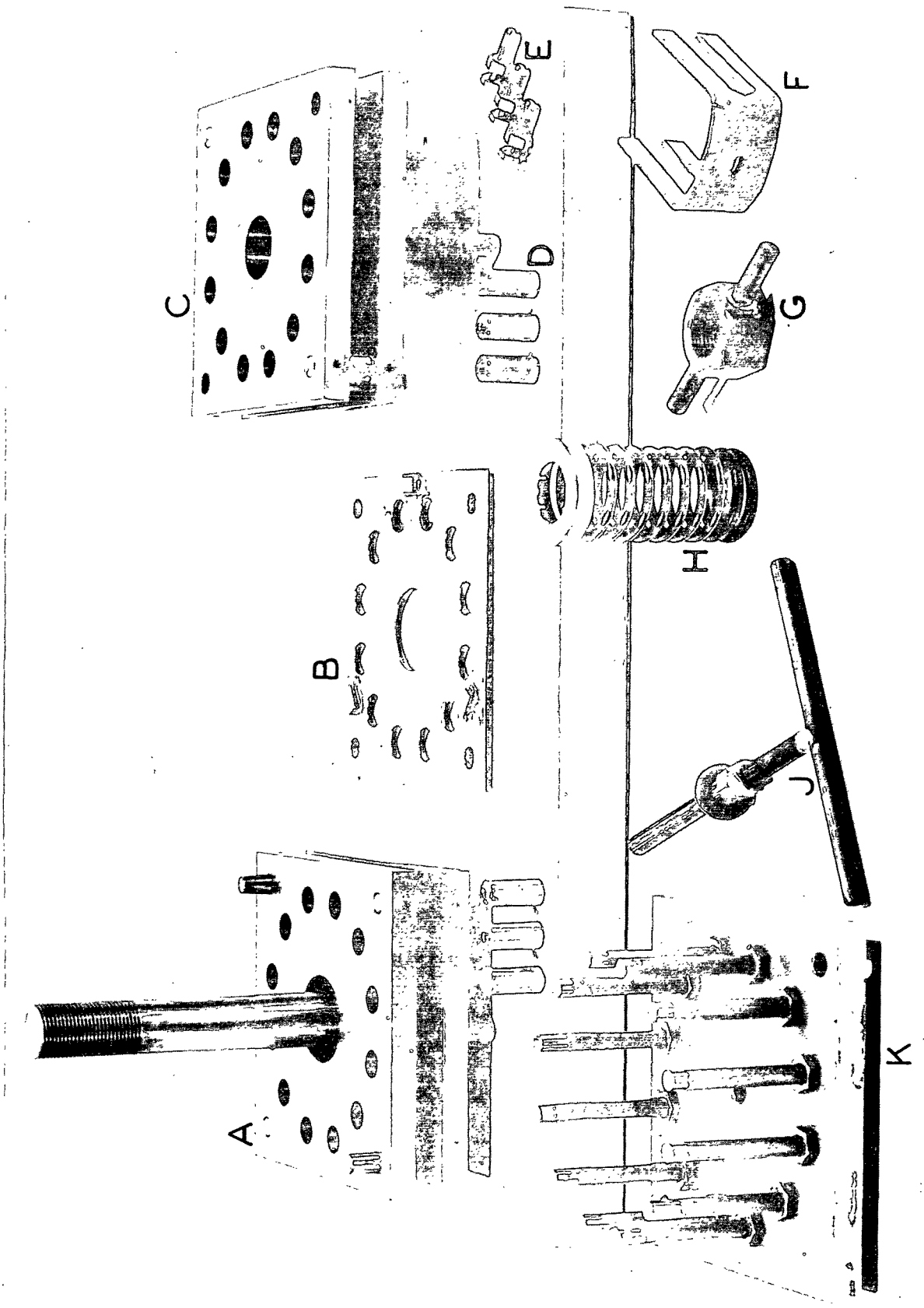

Figure 6

Apparatus for Mounting Samples for the Evaluation of Transverse Tensile Strength:
General Layout of Components

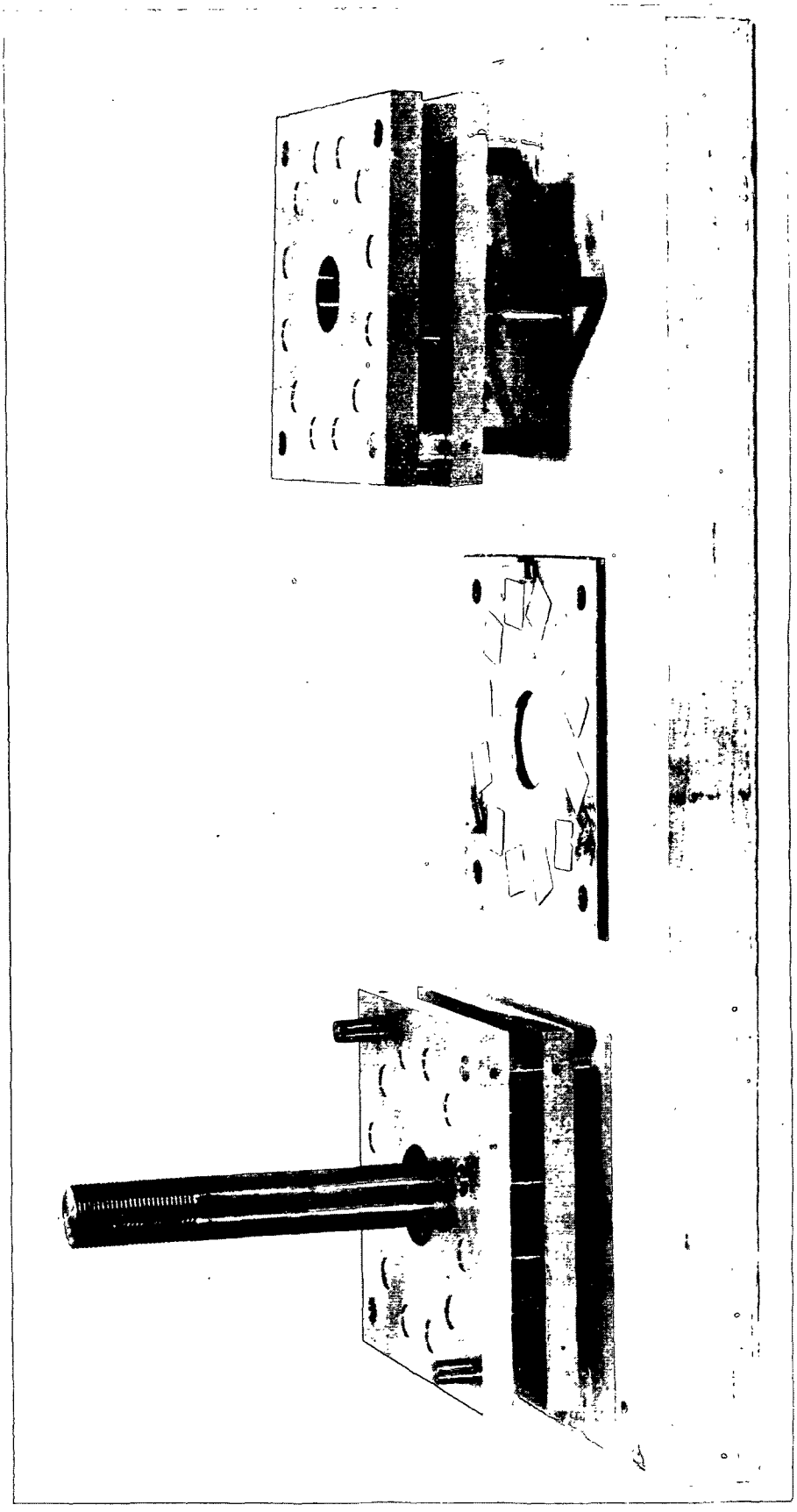

Figure 7

Apparatus for Mounting Samples for the Evaluation of Transverse Tensile Strength:
Ready for the Application of Adhesive to Test Cylinders

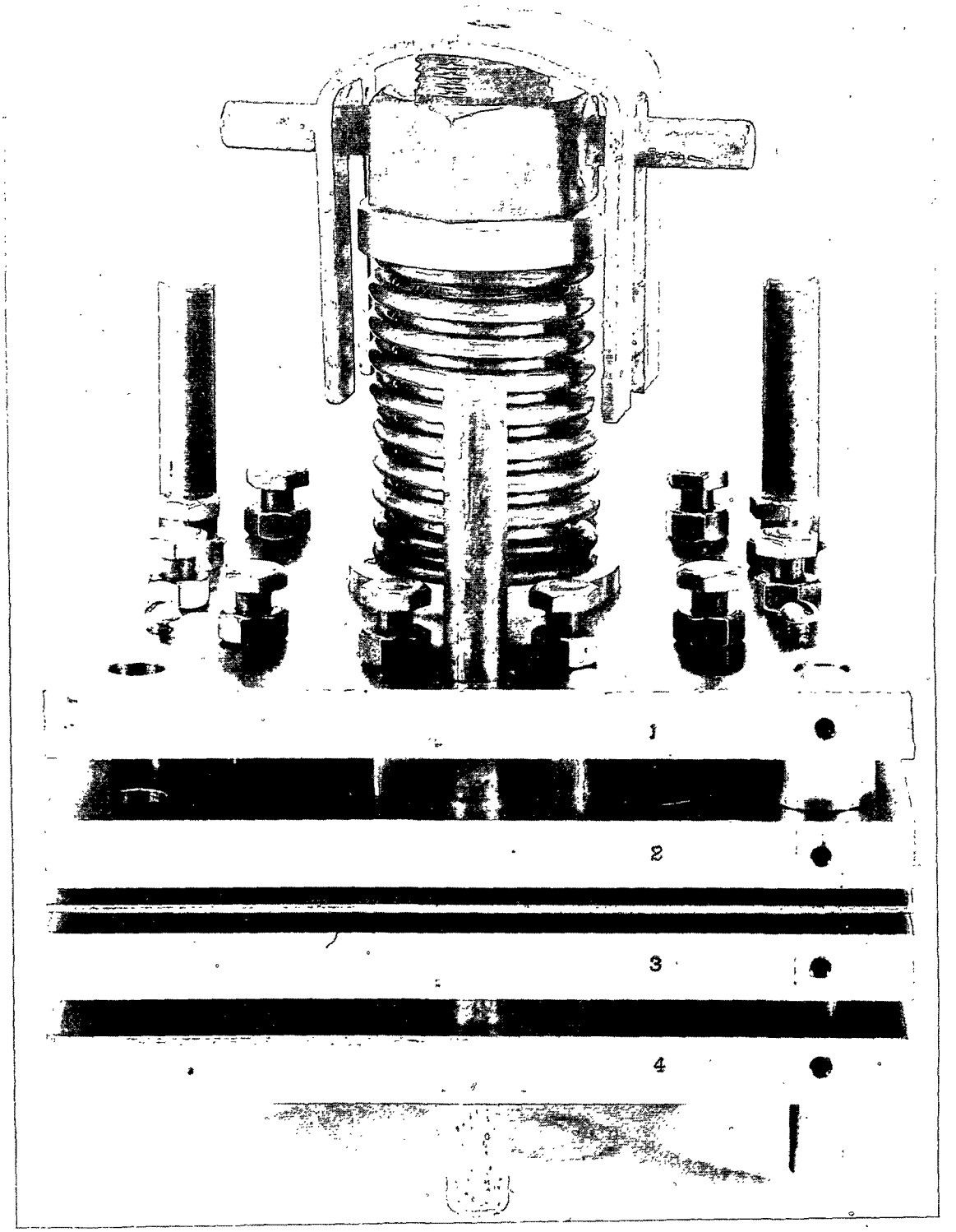

Figure 8

Apparatus for Mounting Samples for the Evaluation of Transverse Tensile Strength: Fully Assembled

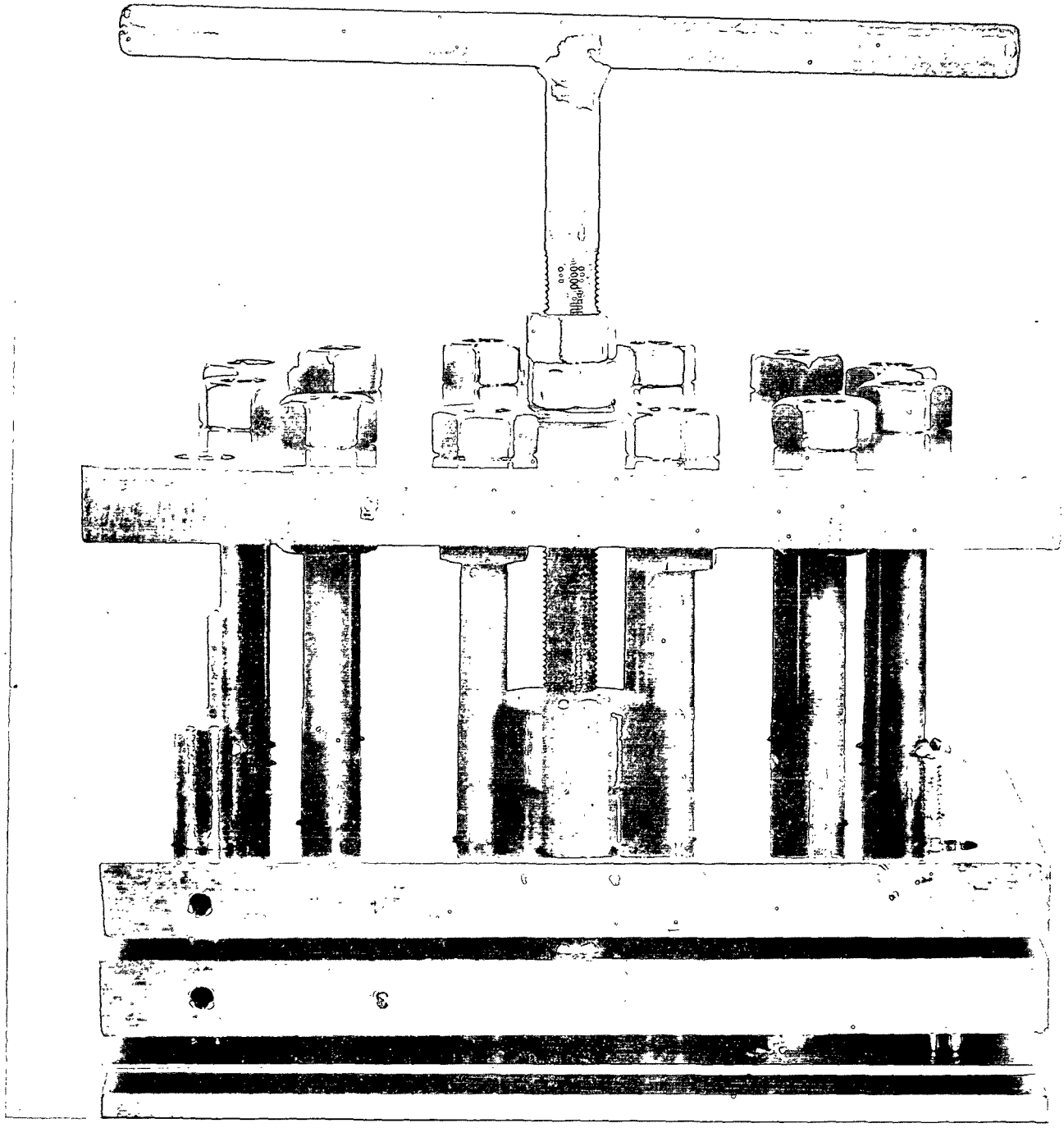

Figure 9

Apparatus for Mounting Samples for the Evaluation of Transverse Tensile Strength: Removal of Test Cylinders

to be doctored onto the test cylinders. The thickness of adhesive is controlled by the position of the ends of the test cylinders below the surface of the apparatus.

After the adhesive has cured to the desired extent, the plate with the samples is placed on the lower half of the apparatus. Then the upper half of the apparatus is inverted and placed on the lower half; aligning pins provide accurate positioning of mating parts. The spring and collar, nut, and yoke are now placed in position on the shaft; but the nut is threaded only part way onto the shaft. The assembled apparatus, shown in Figure 8, is placed in a vacuum desiccator. A rod with a wedge-shaped tip projects into the desiccator through a rubber stopper in the cover and engages the yoke. When the desiccator has been evacuated to the desired absolute pressure, the rod is turned to compress the spring, the deflection of the spring being a measure of the clamping pressure. Plates numbered 1 and 4 apply pressure to the mating test cylinders, while plates 2 and 3 align the cylinders. The top and bottom surfaces of plates 1 through 4 were ground flat on a surface grinder.

When the adhesive has been cured (2 hours at 74°C.), the yoke, nut, spring, and cap screws are removed; and the apparatus is inverted. The ejector is positioned with its twelve spokes passing through plate 4 and resting on the ends of the test cylinders, as in Figure 9. Threading the "T" crank into the end of the shaft forces the twelve test cylinders out of the lower half of the apparatus. The test cylinders are separated from the upper half by driving them out individually

using a rubber-tipped rod and a small mallet (in an improved technique a special pair of pliers is used to press out the cylinders, thus avoiding impact stresses on the mounted samples).

Testing Samples

To apply a uniform tensile stress accurately parallel to the axis of the test cylinders the device shown in Figure 10 was constructed. Two of these devices are required, one to connect each side of the mounted specimen to the jaws of the tensile tester (Baldwin-Southwark or Instron).

When the test cylinder is threaded onto the stud (A) firmly against the faced end of the rod (B), the axes of the test cylinder and the rod are congruent. The precision ball bearing (C), centered on the axis of the rod, is retained by the screw (D) and rests in a shallow hole in the bar (E). Bar (E) is mounted in the yoke (F) which is connected through bolt (G) to the block (J). The bolt provides rotational and axial freedom for attaching and detaching test cylinders when the block is clamped in the jaws of the tensile tester.

GENERAL PROCEDURE OF TTS TEST

To summarize the test, the general procedure is described as follows (the detailed procedure is given in Appendix II):

1. Prepare the specimens of coating.

2. Stir the activator into the epoxy resin and apply the adhesive to the test cylinders positioned in the apparatus for mounting samples.

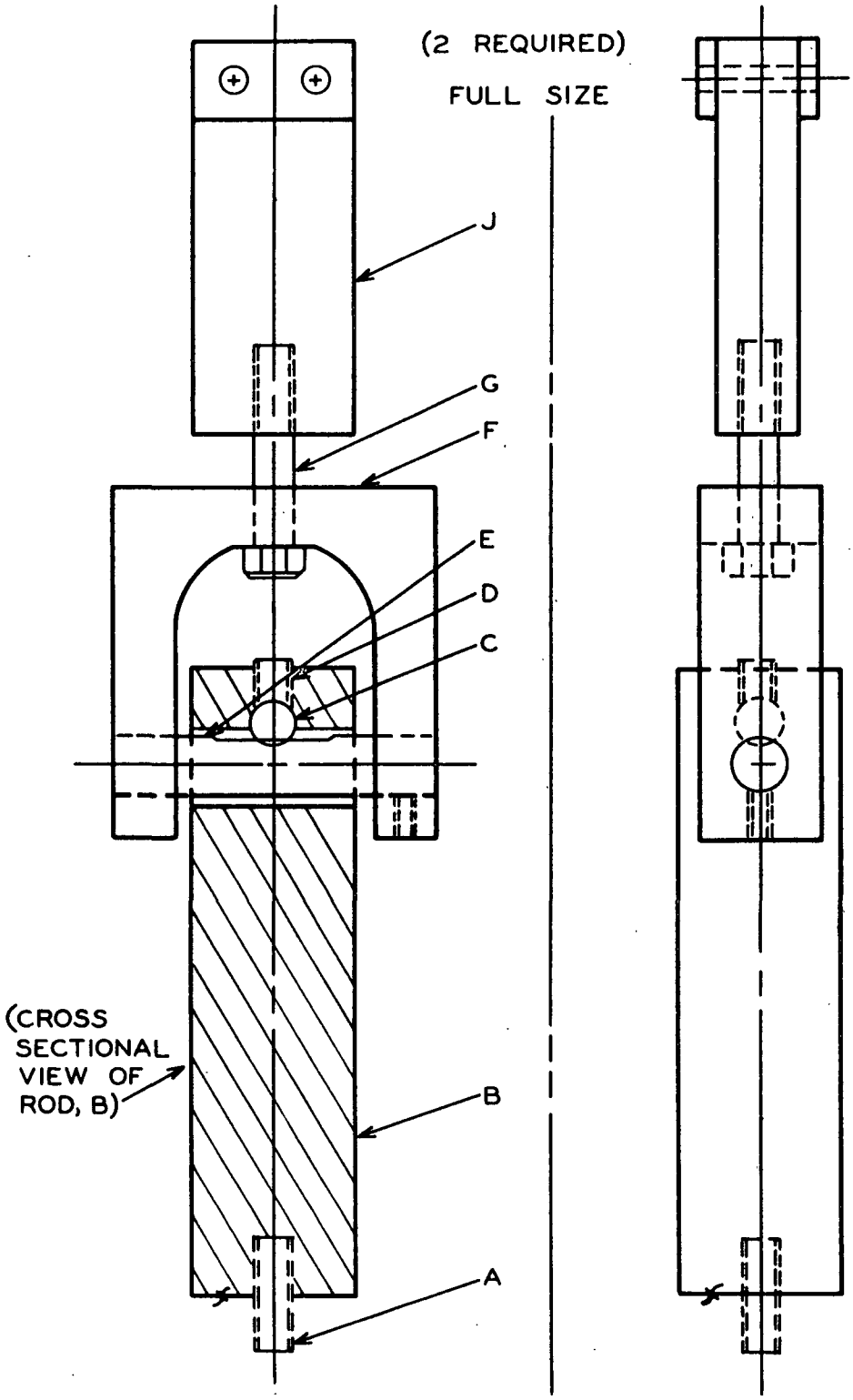

Figure 10. Device for Aligning Test Cylinders during Transverse Tensile Test

3. When the adhesive has cured to the desired degree, assemble the apparatus and place it in a vacuum desiccator.

4. Evacuate the desiccator and clamp the specimens.

5. Remove the assembled apparatus from the desiccator and cure the adhesive in an oven for two hours at 74°C.

6. Remove the test cylinders from the apparatus and carefully trim the edges of the specimens and the adhesive flush with the walls of the test cylinders.

7. Attach the mounted specimens to the aligning devices in the tensile tester (Baldwin-Southwark) and test at a load rate of 500 lb./min.

8. Examine the fractures with a dissecting microscope to estimate visually the location of failure.

9. Quantitatively remove the samples of coating from the test cylinders to determine the extent of adhesive penetration and the location of failure.

TTS TEST VARIABLES

Adhesive Penetration

The penetration of adhesive into the sample is important since the validity of the test is affected. The adhesive must make complete contact with the surface of the sample to avoid local stress intensifications but must not penetrate an undue distance into the sample. The method of analysis for adhesive penetration is described in the next section, but at this point it is desired to discuss the test variables affecting penetration.

There are three test variables affecting adhesive penetration: (1) the time for the preliminary cure of the adhesive before clamping, (2) the clamping pressure, and (3) the thickness of the adhesive layer on the test cylinders. Longer preliminary cure times increase the viscosity of the adhesive and reduce its tendency to penetrate the sample. After about one hour the adhesive is tacky to the touch but does not adhere to the finger when the finger is withdrawn. For bonding to porous samples, preliminary cure times of one hour and two minutes or one hour and 46 minutes were used, depending on penetration desired.

Higher clamping pressures tend to increase penetration. Pressures of four or 12 lb./in.^{2} were used, again depending on penetration desired.

The thicker the adhesive film, the lower is the penetration for a given preliminary cure time and clamping pressure. A constant adhesive thickness of about 0.020 in. was used.

In the evaluation of the TTS of isolated coating it was found desirable to test each coating under two degrees of penetration. The first condition involved negligible penetration, less than 1 lb./ream (25 x 38 in.--500 sheets) by weight or 1 micron in depth, and was obtained with a preliminary cure time of one hour and 46 minutes and a clamping pressure of four lb./in.^{2}. The second condition of one hour and two minutes preliminary cure time and 12 lb./in.^{2} clamping pressure caused the adhesive to penetrate the coating about one to two lb./ream by weight and tended to strengthen the surface layers of the coating.

Conditioning of Samples

To determine the effect of relative humidity on TTS, samples were conditioned for 48 hours over saturated salt solutions of lithium chloride, magnesium nitrate, and potassium chromate which, according to Wink and Sears (32), produce relative humidities of 11, 52, and 86%, respectively, at a temperature of 80°F.

The results are given in Appendix IV and summarized in Table III. No significant difference due to relative humidity is revealed by these data. There are two possible explanations: (1) The coating has been solvent exchanged with ethyl acetate in the isolation procedure so that the coating is plasticized by ethyl acetate rather than water. (2) The samples are all exposed briefly to the same vacuum (about 8 cm. Hg absolute pressure) before clamping, during which process the samples come to about the same final moisture content.

For this study the important fact is that TTS is relatively independent of the relative humidity at which samples are conditioned prior to testing.

Absolute Pressure at Clamping

With a relatively nonporous coating it was considered desirable to check the possibility of air being trapped between the epoxy adhesive and the coating. The results given in Appendix IV and summarized in Table IV suggest that precision was improved by clamping in a partial vacuum, even though the level of TTS was about the same; therefore, all other coating samples were mounted in a partial vacuum of about 8 cm. Hg absolute pressure.

TABLE III

TTS. VS. RELATIVE HUMIDITY

Coating 12MA[a]

Coat weight = 20±5[b] lb./ream

Relative Humidity, %	TTS, lb./in.^{2}
11	2270 ± 120[c]
52	2200 ± 100
86	2210 ± 180

[a] The coating symbols are explained in the Glossary, page 22.

[b] For coat weight, the confidence limit given indicates distribution and is twice the standard deviation of the individual.

[c] For TTS, the confidence limit given indicates precision and is twice the standard deviation of the mean.

TABLE IV

TTS VS. GAS PRESSURE AT CLAMPING

Coating 12MH

Gas Pressure at Clamping, cm.Hg	Coat Weight, lb./ream	TTS, lb./in.^{2}
75 (atmospheric)	14 ± 4	1480 ± 150
8	13 ± 3	1350 ± 50

Rate of Loading

Brittle materials have been shown to have ultimate strengths relatively insensitive to the rate of loading in the range of 40 lb./in.^{2}/sec. (500 lb./min. = 42.5 lb./in.^{2}/sec. for this test). McHenry and Shideler (33) demonstrated a weak dependence for concrete tested in compression; increased rates of loading gave greater strengths. Dietz and McGarry (34) found relatively hard and rigid adhesives, such as phenolic and epoxide types, to have shear strengths independent of the rate of loading from 10 to 10^5 lb./in.^{2}/sec. For glass rods tested in straight tension, Ritland (35) reported a slight increase in breaking strength with increased rates of loading in the range of 1 to 100 lb./in.^{2}/sec.

The clay-starch coatings in this study behave essentially like brittle materials; failure occurs with very little elongation and without noticeable yielding. To verify the effect of rate of loading on TTS, samples were tested at 100, 500, and 1000 lb./min. The results, given in Appendix IV and summarized in Table V, indicate only a slight dependence, if any, of TTS on rate of loading for the range 100 to 1000 lb./min. All further testing was, therefore, carried out at 500 lb./min.

Coating Reproducibility

The reliability of the TTS test and the reproducibility of the coating preparation procedure are suggested by the data given in Appendix IV and summarized in Table VI for two coatings prepared at different times but by the same formula.

TABLE V

TTS VS. RATE OF LOADING

Coating 12MA

Coat weight = 24 ± 1 lb./ream

Rate of Loading, lb./min.	TTS, $lb./in.^2$
100	2400 ± 200
500	2310 ± 50
1000	2450 ± 60

TABLE VI

COATING REPRODUCIBILITY

Coating 12MA

Coating Color, number	Coat Weight, lb./ream	TTS, $lb./in.^2$
E-5807	30 ± 3	2390 ± 150
E-5901	20 ± 5	2220 ± 70

Considering the difference in coat weight the agreement is good.

ADHESIVE PENETRATION AND LOCATION OF FAILURE

VISUAL

It is possible to estimate visually the depth of adhesive penetration and the location of failure in the TTS test described above. The thickness of the isolated coating is measured with a microscope at 100 diameters magnification using an eyepiece micrometer. After the coating is bonded to the test cylinders, the unpenetrated thickness which is

still white, whereas the adhesive-penetrated layer is reddish-brown, is also measured with the microscope. Finally, after the sample has been tested, portions of adhesive and coating on each side of the failure are removed from the test cylinders with a razor blade and examined. The thickness of coating on each side of the failure is measured for a given place on the original sample to locate the failure within the coating.

GRAVIMETRICAL

For quantitative data a material balance is carried out on the sample before and after the TTS has been measured. Since the samples of isolated coating are cut to size with a circular hole cutter, 18 mm. diameter, the initial coat weight is easily determined by weighing the samples to the nearest 0.1 mg. For samples weighing between 7 and 12 mg., the accuracy is better than 2% and probably as good as the uniformity of the coating.

After the TTS test, the coating on the substrate side of the failure is transferred to a tared beaker by brushing with a camels' hair brush frequently re-wet with water. After all the visible coating is brushed into the beaker, liquid remaining on the test cylinder is rinsed with a fine stream of water into the same beaker. This procedure is repeated for each replicate, usually twelve, of a given set of samples.

Similarly, the coating on the air-surface side of the failures is transferred quantitatively to a tared beaker. The beakers are placed in an oven at 95°C. and evaporated to dryness. The weight of coating

recovered is determined to the nearest 0.1 mg. For twelve replicates the depth of penetration can be measured with an accuracy of about 2%. The location of failure, if in a well-defined zone, can be determined to within 2 lb./ream. When the failure occurs randomly or in a broad zone, the exact location of the failure is of minor significance.

NET ADHESIVE RATIO

The net adhesive ratio, which is defined as the adhesive ratio (parts starch/100 parts pigment) of the coating layer after drying, is found by weighing a 20 to 30 mg. sample of isolated coating to the nearest 0.1 mg., extracting the starch, and determining the extracted starch colorimetrically with iodine. The clay is calculated by difference, after correction for volatiles in the coating.

This colorimetric method for starch is a modification of one described by Browning, Bublitz, and Baker (36) for starch in paper. The weighed sample of coating is placed in a 50-ml. beaker. A few drops of distilled H_2O are added and the coating macerated thoroughly with a rubber-tipped stirring rod. The stirring rod is rinsed off into the beaker. Distilled water is added to make a total volume of about 10 ml., and the beaker is placed on a steam bath and heated for 30 min. When the beaker has cooled, 1 ml. concentrated hydrochloric acid and enough distilled water to make 25 ml. total volume are added. The beaker is allowed to stand for an hour while the clay settles. The contents of the beaker are then transferred to a fine-porosity fritted-glass crucible.

The coating is then washed successively with (1) a few milliliters hot, distilled water, (2) 2 ml. 21% hydrochloric acid, (3) 2 ml. 21% hydrochloric acid, (4) 1 ml. concentrated hydrochloric acid diluted with 10 ml. distilled water after 1 minute, and finally (5) a few milliliters of hot, distilled water again. The filtrate is transferred quantitatively from the filter flask to a 100-ml. volumetric flask. Five milliliters of concentrated hydrochloric acid and 2 ml. of iodine reagent are added to the flask, and then distilled water is added up to the mark. The contents are mixed by vigorously inverting the flask ten times. After at least 15 minutes but not longer than one hour the optical density of the solution is determined at 580 mmu wavelength. A Bausch and Lomb Spectronic "20" colorimeter was used.

The iodine reagent consists of 7.5 g. potassium iodide and 5 g. iodine, diluted with distilled water to exactly 500 ml.

A calibration curve for Stayco M starch is given in Figure 11 based on the calibration data given in Appendix V. A starch sample of 0.200 g. ovendry Stayco M was heated in 100 ml. distilled water for 30 minutes on a steam bath and then diluted to 500 ml. in a volumetric flask. The starch concentration in the flask was then 0.400 mg./ml. Aliquots containing the desired amount of starch were pipetted into 100-ml. volumetric flasks. Nine milliliters concentrated hydrochloric acid and 2 ml. iodine reagent were added, and the flask was filled to the mark with distilled water. The flask was mixed and the optical density determined as described above for the coating sample.

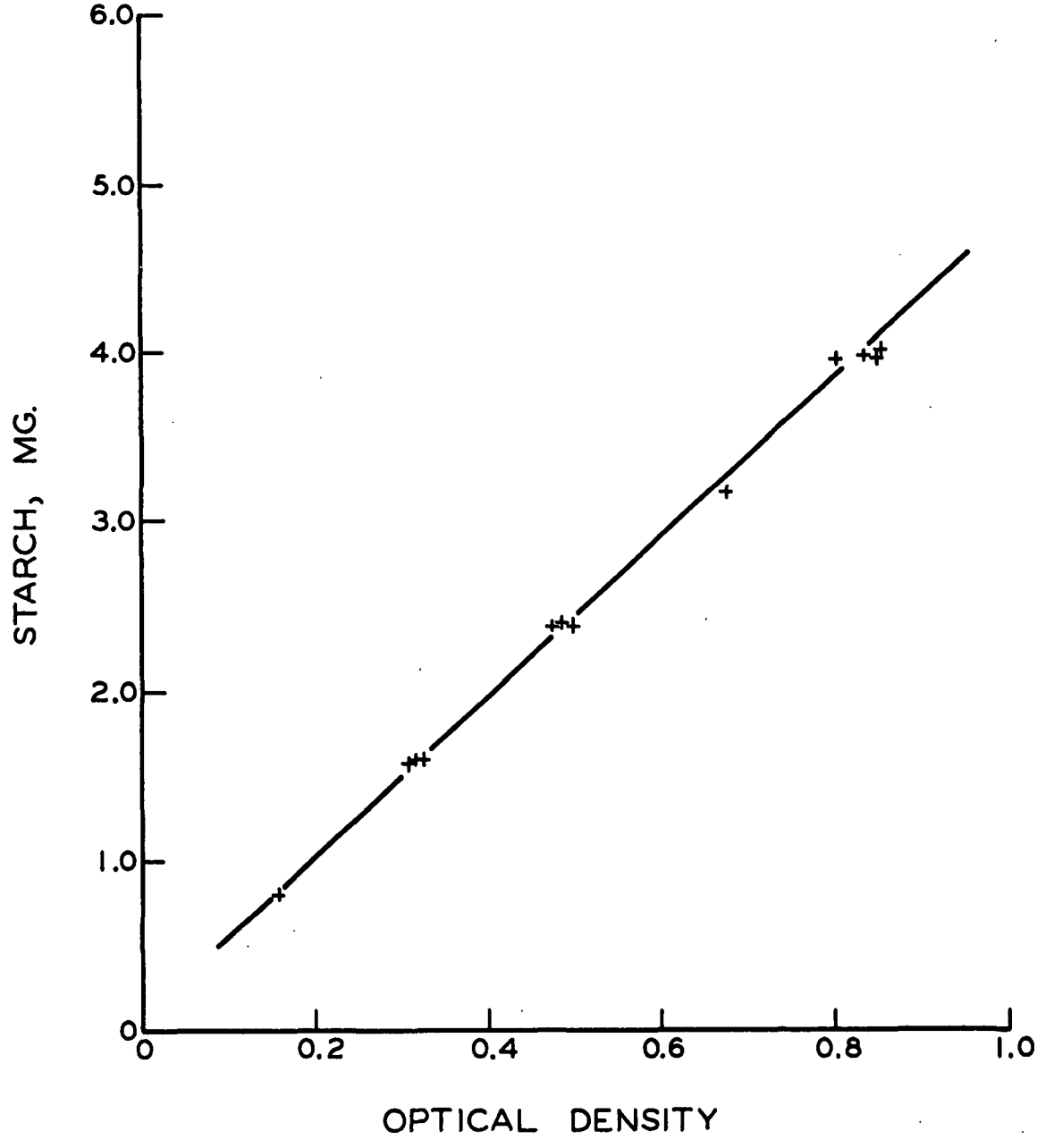

Figure 11. Calibration Curve for Stayco M Starch
(Colorimetric method using iodine)

The accuracy of the starch determination is about 2%. The initial weight of the coating sample is determined with an accuracy of about 1%. The solids content of the various coatings in this study varied from 98.4 to 99.5%. An average solids content of 99.0% was assumed in calculating the clay by difference. Table VII summarizes results given in Appendix VI for four coatings that were applied to Kodapak, so that no adhesive was lost by penetration into the substrate. The coatings were isolated from Kodapak by the same ethyl acetate treatment used for coatings on "MF". The over-all accuracy of the adhesive ratio determinations was about 2%, whereas the precision for four replicates was about 1%.

TABLE VII

ACCURACY AND PRECISION OF ADHESIVE RATIO DETERMINATION

Coating	Initial Adhesive Ratio	Experimentally Determined Adhesive Ratio (4 replicates)	Error, %
10MK	10.0	9.80±0.10	2.0
12SK	12.0	11.98±0.08	0.2
12LK	12.0	12.26±0.26	2.2
14MK	14.0	13.58±0.06	3.0
		Av. precision = 1%	Av. accuracy = 2%

EXPERIMENTAL RESULTS AND DISCUSSION: THE EFFECTS OF CERTAIN VARIABLES ON COATING TTS

The TTS and net adhesive ratio data for all the coatings summarized in this section are given in Appendices IV and V.

PIGMENT PARTICLE SIZE

Three coatings, identical except for the particle size fraction of clay used, were applied to "MF", type VC, and to aluminum foil. The three clay fractions are described in the section above on materials and are identified as S (0.0-0.5 mu), M (0.5-1.0 mu), and L (1.0-2.0 mu). The initial adhesive ratio was 12, and the coatings were dried by natural convection at 73°F.

Hemstock and Swanson (4) have demonstrated that pick strength is unrelated to pigment surface area or particle size for clay-starch coatings on aluminum foil. The results of the coatings on foil, summarized in Table VIII, indicate that TTS is also independent of pigment particle size for coatings on nonporous substrates.

The low TTS values for 12MF may be due to (1) adhesive migration and/or (2) particle alignment. Since coating 12MF was inadvertently dried at a much lower relative humidity than the other coatings[1], the driving force for evaporation of water at the surface of the coating was greater. As Dappen (21) has shown and as will be shown again later in this study, increased rates of drying tend to cause adhesive to

[1] Because of equipment failure in the constant humidity room.

TABLE VIII

TTS VS. PIGMENT PARTICLE SIZE

Coatings on Aluminum Foil

Coating	Pigment Particle Size, mu	Average Coat Weight, lb./ream	TTS, lb./in.^{2}	Location of Failure in Coating
12SF	0.0-0.5	28	2060±140	Random
12MF[a]	0.5-1.0	16[b]	1400±400[b]	Near foil on thick ctgs., random on thin ctgs.
12LF	1.0-2.0	27	2070±90	Random

[a] This coating was dried at less than 10% relative humidity, whereas the other two coatings were dried at 50% relative humidity.

[b] There were large variations in coat weight among the samples in this set. Thin coatings gave high TTS values, thick coatings gave low TTS values.

migrate toward the surface zones of evaporation. For coatings on foil, migration due to drying can proceed only away from the foil-coating interface and toward the air surface. It is significant that thinner coating samples failed randomly within the coating and at higher strength, whereas thicker samples failed near the foil at lower strengths. The layer weakened most by adhesive depletion due to migration would be expected to occur at the foil-coating interface. Also, adhesive migration effects would be expected to be more pronounced in thicker coatings than in thin coatings.

Greater particle alignment may be associated with greater adhesive depletion by a closer packing of the platelets. The ability of the clay particles to assume a close-packed arrangement may be greater for the 0.5-1.0 mu fraction than for the other two fractions. Kraske (17) found that the largest clay fraction had poorer particle orientation than the other two fractions for coatings on MF, type HA. The data were not conclusive on the two smaller clay fractions but seemed to indicate that the medium fraction, 0.5-1.0 mu, had the greatest degree of orientation of the three fractions.

If increased particle alignment could result in a zone of weakness, it would suggest that present concepts of coating strength may need revision. For example, it has been suggested by Hemstock and Swanson (4) that very perfect particle alignment is responsible for strong void-free coating adjacent to the foil surface. The implication seems to be that clay and starch make equal contributions (on a volume basis) to strength so that denser coatings are inherently stronger. The results presented above indicate that the volumetric distribution and configurations of the starch are of primary importance and that replacement of starch by clay, volume for volume, weakens the coating.

If particle orientation induced by the substrate were the primary cause of the weakness in coating 12MF, it would seem reasonable to expect that TTS would be independent of coat weight or thickness. Since TTS varied markedly with coating thickness, adhesive migration due to drying forces is the more plausible explanation; particle orientation, if a factor, would be a result of the adhesive redistribution rather than the cause.

The results for the coatings on a porous substrate, coatings 12VS, 12MV, and 12LV, are summarized in Table IX and shown graphically in Figure 12. By the nature of the TTS test it is impossible to measure the strength at the actual surfaces of the coatings, although the surface strength may be approached very closely. Because of this inherent limitation, the TTS profiles of the coatings are drawn only for that portion of the coating not impregnated with the epoxy adhesive during the TTS test. The TTS of the layers of the coating where failure did not occur can be estimated indirectly as greater than that of the zone of failure. The dashed line is given to indicate a minimum TTS for that location in the coating; the actual TTS may be much greater.

TABLE IX

TTS VS. PIGMENT PARTICLE SIZE

Coating	Pigment Particle Size, mu	Net Adhesive Ratio	Coat Weight, lb./ream	Coat Weight Penetrated, lb./ream	TTS, lb./in.^{2}	Location of Failure in Coating, % of coat wt. from sub.-ctg. interface [a]
12SV	0.0-0.5	9.8	25±2	(negligible)	1690±80	(near sub. or random)
			25±3	"	1740±190	"
			23±5	0.4	2180±40	(random)
12MV	0.5-1.0	9.5	24±6	< 1	1760±60	(near sub. or random)
			27±9	3.4	1940±40	"
12LV	1.0-2.0	9.8	24±3	< 0.7	1180±80	20
			24±3	3.4	1620±60	36

[a] Sub.-ctg. means substrate-coating.

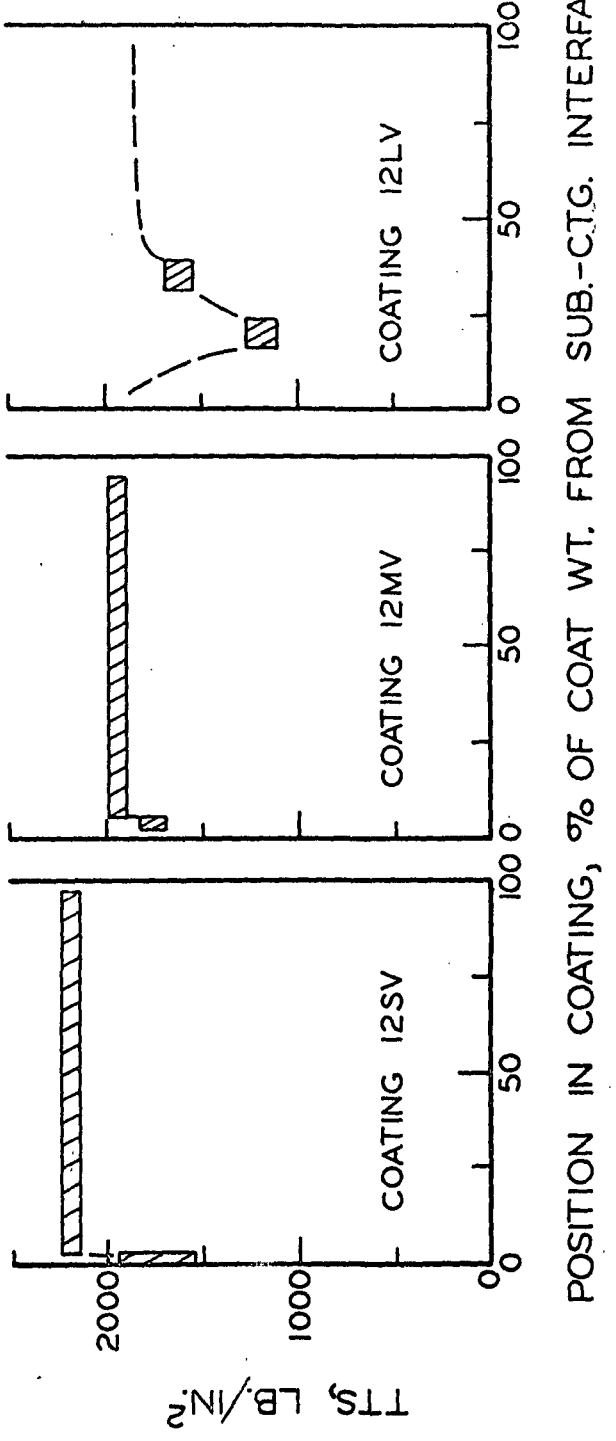

Figure 12. TTS vs. Pigment Particle Size

The cross-hatched rectangle shows two things about the coating: (1) The position of the failure is indicated with an accuracy of about 2 lb./ream by the horizontal position and width of the rectangle. (2) The TTS is shown by the vertical position of the rectangle, the height of the rectangle being the 95% confidence limits of the mean.

If the behavior of the central 90% of the coating is taken as a criterion, there seems to be a definite relationship between TTS and pigment particle size; the TTS increased as the particle size decreased. The layers of coating adjacent to the substrate in 12SV and 12MV have about the same TTS; this suggests that the strength of these layers is dictated primarily by the substrate and its effect on vehicle penetration.

Coating 12LV, with the largest clay fraction, behaved in a distinctly different manner than did the coatings having the smaller clay fractions. Failure occurred in a well-defined zone within the coating. The location of the zone of failure varied with the testing conditions, due perhaps to reinforcement of the coating by penetration of the epoxy adhesive, but was generally about 1/5 to 1/3 the coating weight from the substrate-coating interface.

The explanation that seems most tenable is that in one direction starch has left the zone of weakness due to vehicle penetration of the substrate and in the other direction starch has migrated with the vehicle toward the air surface and/or become immobilized before it could be drawn toward the substrate. The resulting zone of depleted starch

content would be expected to be lower in strength than adjacent zones having more starch. There is a striking connection between this explanation and Kraske's (17) pore structure analysis for this large particle size coating. He visualized this coating having constricted, or ink-bottle shaped, pores in order to explain his pore volume and internal surface area data. He pictured constricted pores with openings of two orders of magnitude in size but had no evidence to suggest a preferential location of either size opening. The zone of weakness revealed by TTS testing would be the logical location of large pores, with large openings probably on the substrate side. The smaller constricted pores could be the interparticle voids opening to the air surface of the coating.

The greater strengths of the smaller clay fractions is explainable on the basis of adhesive retention and distribution. Coating 12SV retained more starch than coating 12MV. The distribution of starch in 12SV and 12MV would appear to be more uniform than in 12LV; thus, the starch in 12LV may not be as effective as an equal concentration in 12SV. On a volume basis, the starch concentration at the zones of failure in 12LV may be less than the starch concentration in 12MV because of the greater void volume found by Kraske (17) in the coating of the largest clay fraction. The importance of volumetric starch concentration is again suggested.

SUBSTRATE PORE SIZE

A coating with the largest clay fraction (1.0-2.0 mu) was applied to aluminum foil and to the three types of "MF" having mean pore sizes

of 0.10, 0.45, and 0.80 mu. The initial adhesive ratio was 12, and the coating was dried by natural convection at 73°F. The results are summarized in Table X. Figure 13 is a graphic portrayal of the coatings on "MF".

The coating applied to foil, 12LF, was stronger than the weak zones of the coatings on porous substrates; however, a large portion of coating 12LA, i.e., the central 50%, is as strong as, or stronger than, the coating on foil. The net adhesive ratio data show that 12LV lost 18% of its original starch by penetration into the substrate, but 12LA and 12LH lost only 5%. If substantial quantities of starch were lost from the zones of weakness, the major portions of 12LA and 12LH must approach the original adhesive ratio much closer than the 5% difference found for the total coating; this would help explain the strength behavior.

The pore sizes and configurations near the coating surfaces probably influence the extent of epoxy adhesive penetration in the TTS test using the shorter preliminary cure time and higher clamping pressure. The greater penetration of 12LA (6.4 lb./ream) compared with 12LH (3.0 lb./ream) indicates that: (1) The coating on the larger pore size substrate has larger pore openings. (2) The epoxy adhesive probably did a more efficient job of reinforcing coating 12LA, thus contributing to the higher TTS obtained.

It would seem appropriate to rank these coatings with regard to TTS by the strengths of the weakest zones. Clearly, the TTS of a clay-starch coating increases with increasing substrate pore size, under the conditions

TABLE X

TTS vs. SUBSTRATE PORE SIZE

Coating	Substrate Pore Size, mu	Net Adhesive Ratio	Coat Weight, lb./ream	Coat Weight Penetrated, lb./ream	TTS, lb./in.^{2}	Location of Failure in Coating, % of coat wt. from sub.-ctg. interface
12LF	(foil)	12.0	27	--	2070±90	(random)
12LV	0.10	9.8	24±3	< 0.7	1180±80	20
			24±3	3.4	1620±60	36
12LH	0.45	11.4	22±2	1.2	1420±90	9
			22±3	3.0	1790±90	14
12LA	0.80	11.4	23±2	(negligible)	1630±70	13
			26±5	6.4	2160±40	24

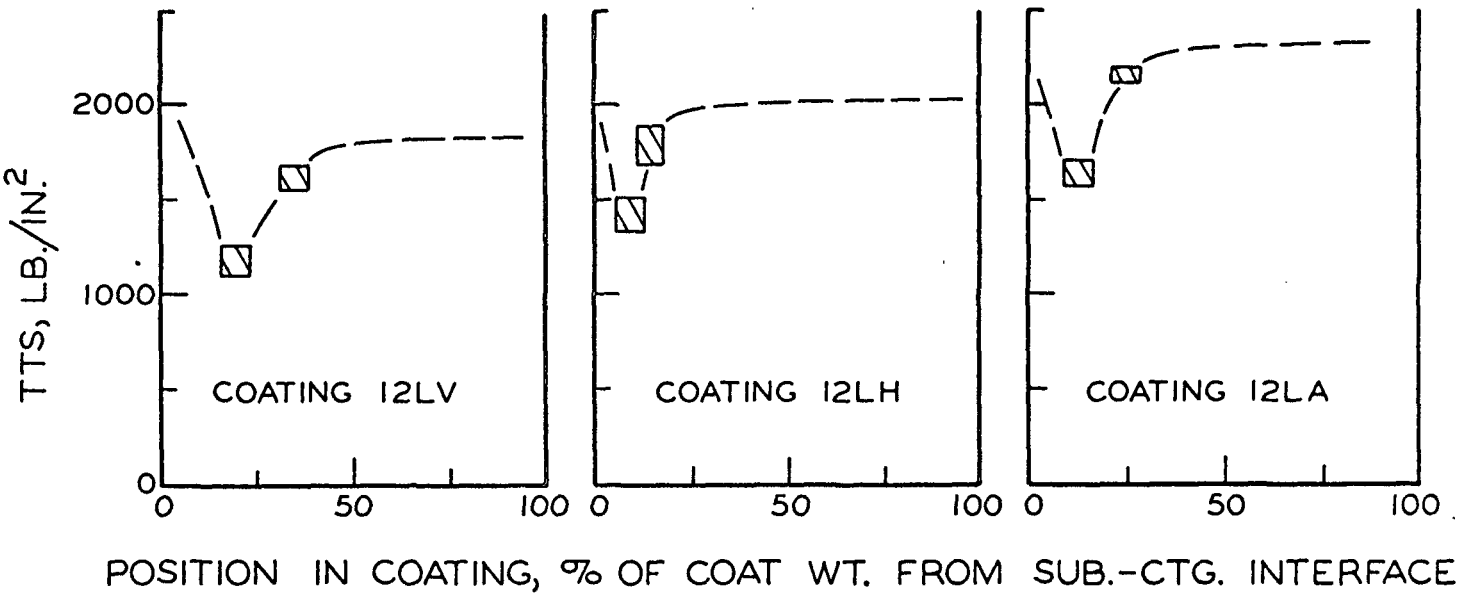

Figure 13. TTS vs. Substrate Pore Size

of this study. At first sight this result seems contrary to the expected behavior. The explanation suggested is as follows:

Poiseuille's Law for laminar flow of liquids in cylindrical capillaries states that

$$\underline{u} = (\underline{r}^2 \underline{\Delta P})/(8 \eta \underline{L}) \qquad (1)$$

where $\underline{u}$ = velocity of flow, cm./sec.

$\underline{\Delta P}$ = pressure difference driving the liquid, g./cm.^{2}

η = viscosity of liquid, poise

$\underline{L}$ = length of liquid column in the capillary, cm.

The driving force for penetration of coating is due to the weight of the coating and capillary attraction. The weight of the coating can be shown to be a negligible factor compared to the capillary attraction. The pressure difference across the meniscus for a liquid wetting a cylindrical capillary is given in Equation (2).

$$\underline{\Delta P} = (2 \gamma \cos \theta)/\underline{r} \qquad (2)$$

where γ = surface tension of the liquid, g./cm.

θ = contact angle between liquid and wall of capillary, radians

Combining Equations (1) and (2)-- $\underline{u} = (\underline{r} \gamma \cos \theta)/(4 \eta \underline{L})$ (3)

The rate of penetration may also be expressed without reference to $\underline{L}$, as shown by Washburn (37). Since $\underline{u} = \underline{dL}/\underline{dt}$, where $\underline{t}$ = time, sec.

$$\underline{dL}/\underline{dt} = (\underline{r} \gamma \cos \theta)/(4 \eta \underline{L}) \qquad (4)$$

Integrating Equation (4) from $\underline{L} = 0$ to $\underline{L} = \underline{L}$ and from $\underline{t} = 0$ to $\underline{t} = \underline{t}$:

$$\underline{L} = (\underline{r} \gamma \cos \theta)^{1/2} \, \underline{t}^{1/2} / (2 \eta)^{1/2} \qquad (5)$$

Differentiating with respect to $\underline{t}$ gives

$$\underline{u} = \underline{dL}/\underline{dt} = (1/2)(\underline{r} \gamma \cos \theta)^{1/2} \, (1/\underline{t})^{1/2} \, (1/2 \eta)^{1/2} \qquad (6)$$

Therefore, for a given coating and substrate material, the velocity of penetration should be directly proportional to the square root of the pore size after a given time of penetration. For substrates of "MF" with similar void fractions but different pore sizes, the volume rate of penetration per unit area of surface coated should vary directly with the square root of the pore size. Thus, near the instant of application the vehicle of coating 12LA penetrates about 1/3 more rapidly than 12LH and nearly three times faster than 12LV. The effects of this difference in rate of penetration seem to be reflected in the structure of the coating. The pigment particles in 12LA were immobilized in a few seconds; visually, the coating was observed to have "set", i.e., lost its wet look. Coating 12LV required a couple minutes to lose its wet look or set. The rate at which pigment immobility is obtained probably affects the density of the coating and the amount of starch retained with the clay.

At a low rate of penetration, the vehicle is visualized as being drawn from the coating layer directly adjacent to the substrate. When this layer has compacted to a rigid structure, vehicle is supplied from a layer farther from the substrate, and so on, until the coating as a whole has set. Vehicle penetration and coating compaction are maximized.

At a high rate of penetration, the vehicle may be withdrawn from the coating so rapidly that the layer adjacent to the substrate could fill the requirement only instantaneously; and the vehicle is almost immediately supplied from the total coating thickness. As vehicle leaves the coating, the pigment particles, and any layers of adhesive

immobilized adjacent to the particle surfaces, coalesce to form a rigid structure. The vehicle flowing between and around fixed or slowly moving clay particles will assume a velocity distribution such that the greatest rate of flow will occur in the center of the channels available for flow. Saturated flow could therefore end while a large portion of the vehicle still exists around the pigment particles.

When saturated flow ends and air enters the coating, i.e., the wet look disappears, vehicle must flow around particles rather than between them; and the resistance to flow becomes much greater. Therefore, it is suggested that the major loss of adhesive to the substrate occurs in the saturated state of flow and that low rates of penetration favor the maintenance of this type of flow, even to the extent that a greater volume of vehicle penetrates a substrate of small pore size than it does a substrate of large pore size.

Another important point is that the small pore can compete more effectively than the large pore in the struggle between substrate and pigment for the vehicle, because the capillary driving force is inversely proportional to pore diameter. A substrate with 0.10 mu pores should exert eight times the driving force of a substrate with 0.80 mu pores. The distribution of vehicle between substrate and pigment must represent an approach to equilibrium between the capillary forces of the two systems.

Cutting 0.5 mu cross sections of coatings such as 12LH and 12LA with a thin-sectioning microtome and examining the extent of starch

penetration by staining with an aqueous iodine solution revealed an enlightening fact. The adhesive had penetrated farther into the substrate with the larger pores than was the case with the smaller pores. This indicates that depth of penetration into the substrate is not proportional to the quantity of adhesive lost from the coating, since coatings on smaller pore size substrates tended to lose more starch. It is not surprising that Casey and Libby (38) did not find a correlation between depth of adhesive penetration into the bodystock and wax pick strength for starch-clay coatings on paper.

The thinner but more concentrated layer of starch found in smaller pore-size substrates may contribute to pick strength by strengthening the substrate-coating bond and the surface layer of the substrate.

INTERACTION: PARTICLE SIZE VS. PORE SIZE

Coatings prepared with the three clay fractions were applied to the three types of "MF" and to aluminum foil. The initial adhesive ratio was 12, and the coatings were dried by natural convection at 73°F. The results presented in the two preceding sections were drawn from this larger set of coatings. It was considered desirable to discuss the effects of pigment particle size and substrate pore size for conditions under which pigment particles could not penetrate the substrate to a significant extent.

The question is inevitably raised, "What happens when pigment particles can and do penetrate the substrate?" The results are summarized

in Table XI, but the easiest way to see the pattern is by means of the graphical representation in Figure 14.

In the previous discussions the vehicle penetrated the substrate and the pigment was left behind. When the pigment also penetrates the substrate, the coating strength and structure are altered markedly. This is evident for the smaller clay fractions on the larger substrate pore sizes (see coatings 12SH, 12SA, 12MH, and 12MA). Minimum TTS values for 12SH, 12SA, 12MH, and 12MA are not too reliable because the roughness of the substrate side of the coating (due to pigment penetration) may have prevented the epoxy adhesive from bonding completely.

The most noticeable difference in these coatings, compared to the coatings without pigment penetration, is the zone of weakness located in the upper third of the coating, i.e., toward the air surface of the original coating. This new zone of weakness follows the same trends of TTS vs. substrate pore size and pigment particle size as were previously described. TTS is higher for the smaller clay fraction and for the larger pore size substrate.

These coatings set quite rapidly and appear to have a more open structure. When the pigment particles are much smaller than the pores, as in coatings 12SA and 12MA, the apparent density as determined by the mercury intrusion method developed by Kraske (17) falls off sharply. Tentative apparent density data available for these coatings are summarized in Table XII. For any given clay fraction there seems to be a trend toward lower densities as substrate pore size increases.

TABLE XI

INTERACTION OF PIGMENT PARTICLE SIZE AND SUBSTRATE PORE SIZE

Coating	Pigment Particle Size, mu	Substrate Pore Size, mu	Net Adhesive Ratio	Coat Weight, lb./ream	Coat Weight Penetrated, lb./ream	TTS, $lb./in.^2$	Location of Failure in Coating, % of coat wt. from sub.-ctg. interface
12SV	0.0-0.5	0.10	9.8	25±3	(negligible)	1740±190	(near substrate or random)
				23±5	0.4	2180±40	(random)
12SH	"	0.45	11.0	24±3	3.1	1340±40	(near sub.)
				23±3	3.7	2230±40	73
12SA	"	0.80	11.3	24±3	3.2	1170±90	(near sub.)
				26±4	3.7	2420±80	73
12MV	0.5-1.0	0.10	9.5	24±6	< 1	1760±60	(near sub. or random)
				27±9	3.4	1940±40	"
12MH	"	0.45	10.7	22±2	< 1	1010±110	(near sub.)
				25±11	1	1360±60	"
				22±3	3	1680±110	"
						2000±200[a]	(near sub. or 2/3 coat wt. from sub.)
12MA	"	0.80	11.2	20±6	< 4	1660±160	(near surfaces)
				20±5	4.3	2220±70	78
12LV	1.0-2.0	0.10	9.8	24±3	< 0.7	1180±80	20
				24±3	3.4	1620±60	36
12LH	"	0.45	11.4	22±2	1.2	1420±90	9
				22±3	3.0	1790±90	14
12LA	"	0.80	11.4	23±3	(negligible)	1630±70	13
				26±5	6.4	2160±40	24

[a] These values were obtained by retesting the portion of coating remaining after the preceding set was tested.

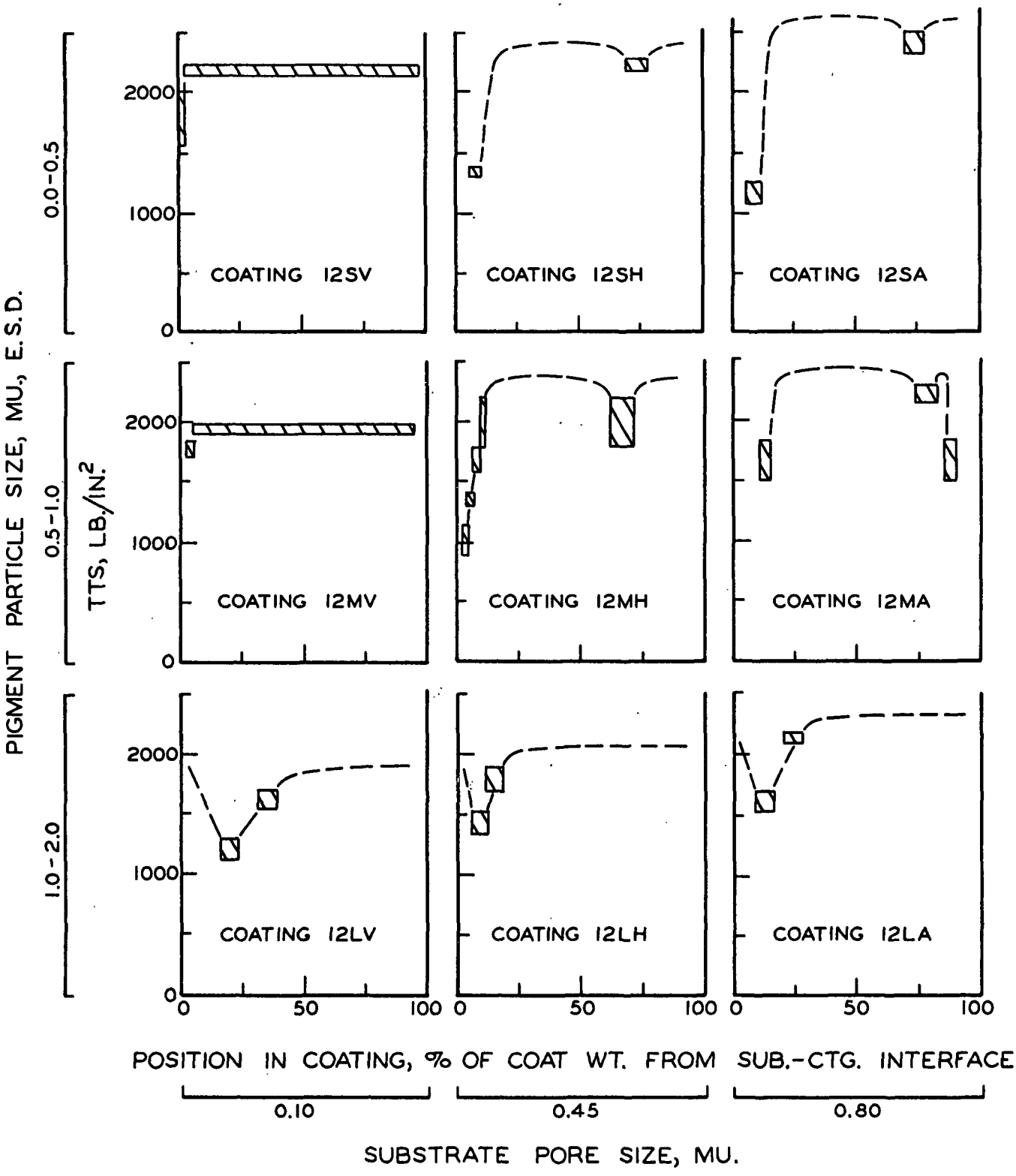

Figure 14. Interaction of Pigment Particle Size and Substrate Pore Size

TABLE XII

APPARENT DENSITY DATA

Coatings on "MF"
Initial adhesive ratio = 12
Dried by natural convection at 73°F.

g./cm.^{3}

Pigment Particle Size, mu, e.s.d.	Substrate Pore Size, mu		
	0.10	0.45	0.80
0.0-0.5	1.54[a]	1.48[a]	1.12[a]
0.5-1.0	--	1.60	1.18
1.0-2.0	--	1.35[a]	1.29[a]

[a] Data provided by D. J. Kraske (39).

The low apparent densities for the 1.0-2.0 mu clay fraction are probably due primarily to poor particle packing rather than pigment penetration.

Table XIII summarizes the net adhesive ratio data for the nine coatings; individual values are in Appendix VI. Substrate pore size seems to be an important factor in adhesive penetration. The adhesive lost by substrate penetration is nearly the same for all three coatings on a given pore-size substrate. The 0.5-1.0 mu clay fraction lost more starch than either of the other two fractions for a given substrate. This may be related to the increased tendency to assume a preferred orientation reported by Kraske (17) for this fraction. It will be recalled that this clay fraction had less TTS than the other fractions in coatings on aluminum foil.

TABLE XIII

NET ADHESIVE RATIO VS. PIGMENT PARTICLE SIZE AND SUBSTRATE PORE SIZE

Coatings on "MF"
Initial adhesive ratio = 12
Dried by natural convection at 73°F.

Pigment Particle Size, mu, e.s.d.	Substrate Pore Size, mu		
	0.10	0.45	0.80
0.0-0.5	9.8	11.0	11.3
0.5-1.0	9.5	10.7	11.2
1.0-2.0	9.8	11.4	11.4

INITIAL ADHESIVE RATIO

Coatings with initial adhesive ratios of 10 and 14 were applied to "MF", type VC, and to aluminum foil. The 0.5-1.0 mu clay fraction was used, and the coatings were dried by natural convection at 73°F. These two coatings are compared in Table XIV and in Figures 15 and 16 with a similar coating, previously described, having an initial adhesive ratio of 12.

The most obvious feature of these coatings is that TTS increased with increasing initial adhesive ratio, or with increasing net adhesive ratio. The data shown in Figure 16 suggests that the relationship between TTS and net adhesive ratio may not be linear for the coatings of "MF". The low significance level of the TTS data for coating 12MF enables one to draw a wide variety of curves to fit within the 95%

TABLE XIV

TTS VS. INITIAL ADHESIVE RATIO

Coating	Net Adhesive Ratio	Coat Weight, lb./ream	Coat Weight Penetrated, lb./ream	TTS lb./in.^{2}	Location of Failure in Coating
10MV	8.1	26±7	0.2	1710±50	Near surfaces or random
		25±6	2.2	1870±30	In broad zone near ctr. of ctg. on air surface side
12MV	9.5	24±6	< 1	1760±60	Near sub. or random
		27±9	3.4	1940±40	" "
14MV	11.3	23±3	0.8	2170±60	Near surfaces
		23±3	2.1	2260-40	Random
10MF	10.0	28	—	1430±150	Random
12MF	12.0	16	—	1400±400	Random on thin, near foil on thick coating specimens
14MF	14.0	24	—	2060±90	Random

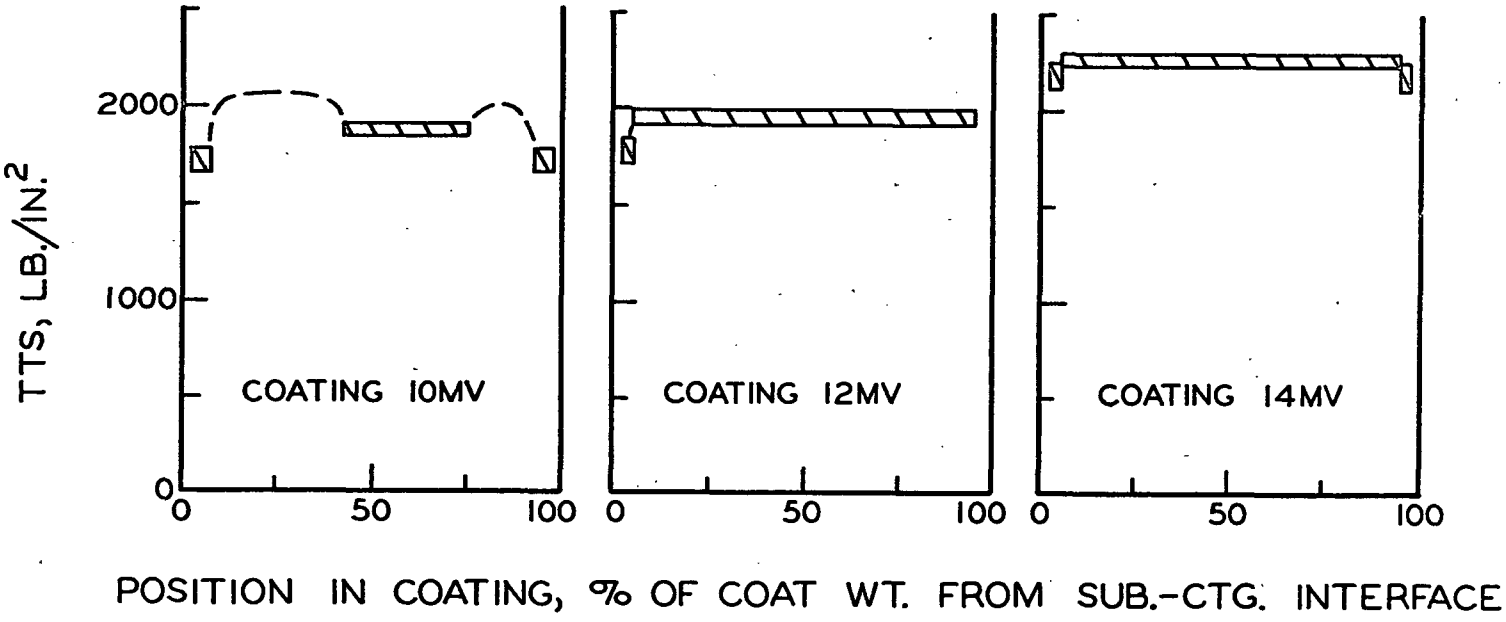

Figure 15. TTS vs. Initial Adhesive Ratio

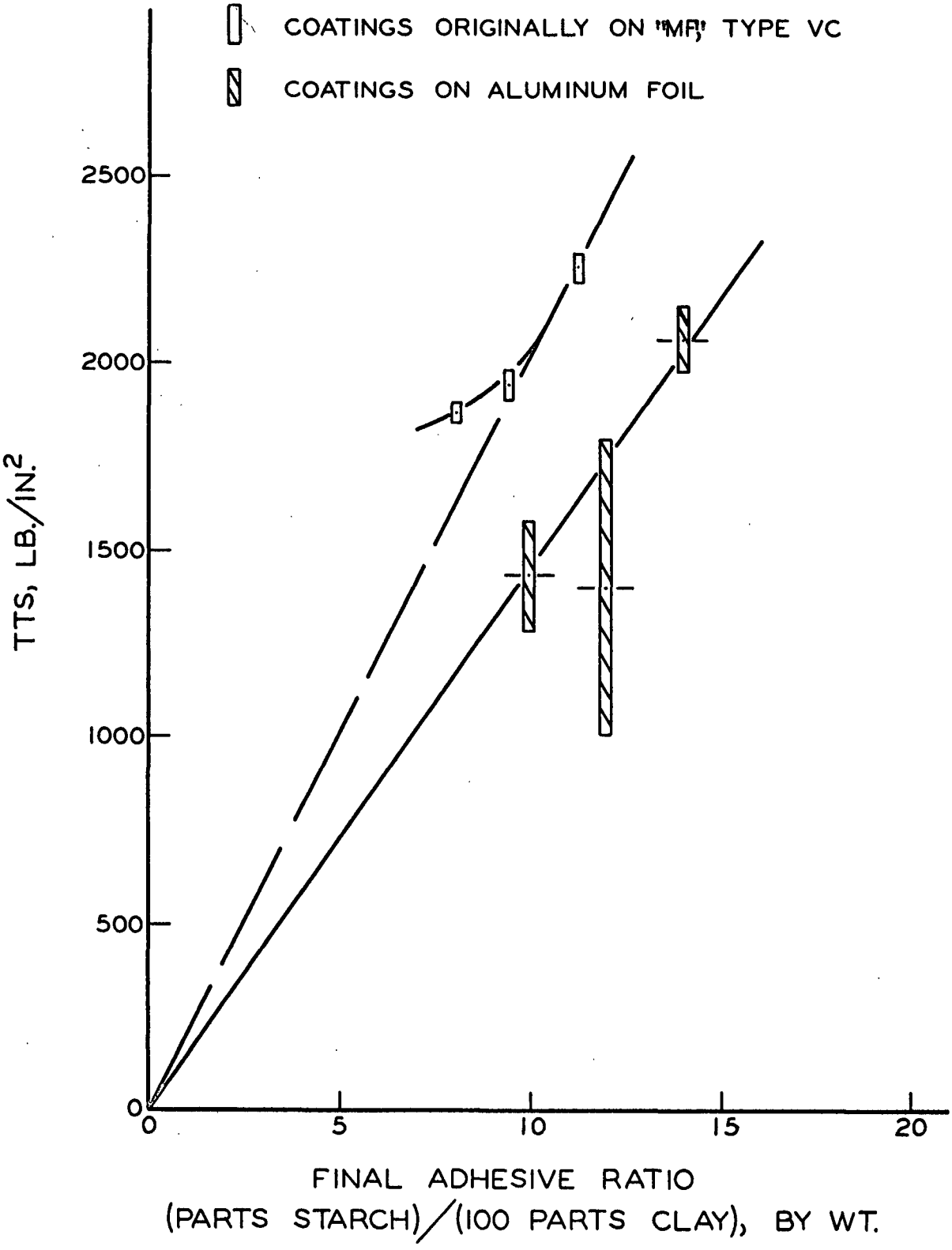

Figure 16. TTS vs. Final Adhesive Ratio

confidence limits. The low relative humidity at which 12MF was dried has been mentioned above as a possible cause of the low TTS of 12MF. It is interesting and perhaps significant that a straight line can be drawn through the origin and the data points for coatings 10MF and 14MF. TTS may be directly proportional to the final adhesive ratio for clay-starch coatings on foil when the adhesive distribution is uniform.

The second feature shown in Figure 16 is that for a given adhesive ratio, the coatings on "MF" have greater TTS than the coatings on foil. This effect is contrary to the findings of Hemstock and Swanson (4) for pick strength. Pick strength as measured with the IPC bonding strength tester, and probably other press simulation tests, is sensitive to the physical properties of the bodystock. This was shown by the following demonstration:

The clay-starch coating (initial adhesive ratio = 12, 0.5-1.0 mu clay fraction, dried in air at 73°F.) was applied to "MF", type HA, and to aluminum foil. Strips of these two coatings, still on their original substrates, were tested with the IPC bonding strength tester using the prefilming technique described by Wink, Shillcox, and Van Eperen (2). The coating on "MF" gave a VVP of less than 10, and on aluminum foil it gave a VVP greater than 60. However, when the coating originally on "MF" was mounted coating side down on aluminum foil with a thin layer of Trim Adhesive (Minnesota Mining & Mfg. Co.) and the "MF" removed with ethyl acetate, the VVP obtained was again greater than 60.

Further consideration of the influence of substrate properties on the pick strength of coated paper is needed. Mere retention of adhesive within the coating or even preferential particle alignment do not insure high TTS, and their influence on pick strength certainly needs closer scrutiny.

METHOD OF DRYING

Drawdowns of coating 14MV were dried by a blast of 200°F. air from a home-type hair dryer, as well as by natural convection at 73°F. Hot air-blast drying required one minute for coatings on "MF" and two minutes for coatings on aluminum foil. The time required was judged by the changes in appearance of the coating. The coating lost its wet look, or set, fairly quickly; but more time was needed for the coating to develop the ivory color characteristic of the dry coating (the wet coating was more tan-colored than ivory). The ivory end point was used for the hot air-blast drying.

The results are summarized in Table XV and in Figure 17. It should be reemphasized that the dashed portion of the TTS curves is an approximation of the minimum possible TTS. The actual TTS may be much greater, but not much less, than the dashed line. This limitation must be constantly borne in mind when comparing the various coatings by means of the figures.

The increased rate of drying reduced the TTS of both the coating on "MF" and the one on aluminum foil. The coating on foil lost a much larger portion of its TTS than did the coating on "MF". Apparently, the

TABLE XV

TTS VS. METHOD OF DRYING

Coating	Method of Drying	Substrate Pore Size, mu	Net Adhesive Ratio	Coat Weight, lb./ream	Coat Weight Penetrated, lb./ream	TTS lb./in.^{2}	Location of Failure in Coating, % of coat wt. from sub.-ctg. interface
14MV	Natural convection at 73°F.	0.10	11.3	23±3	0.8	2170±60	(near surfaces)
				23±3	2.1	2260±40	(random)
$14MV_{HAB}$	Hot air blast at 200°F.	"	12.4	22±3	0.3	2020±80	17
				23±6	0.7	2030±60	14
14MF	Natural convection at 73°F.	(foil)	14.0	24	--	2060±90	(random)
$14MF_{HAB}$	Hot air blast at 200°F.	"	"	31	--	600±300	(narrow zone adjacent to foil)

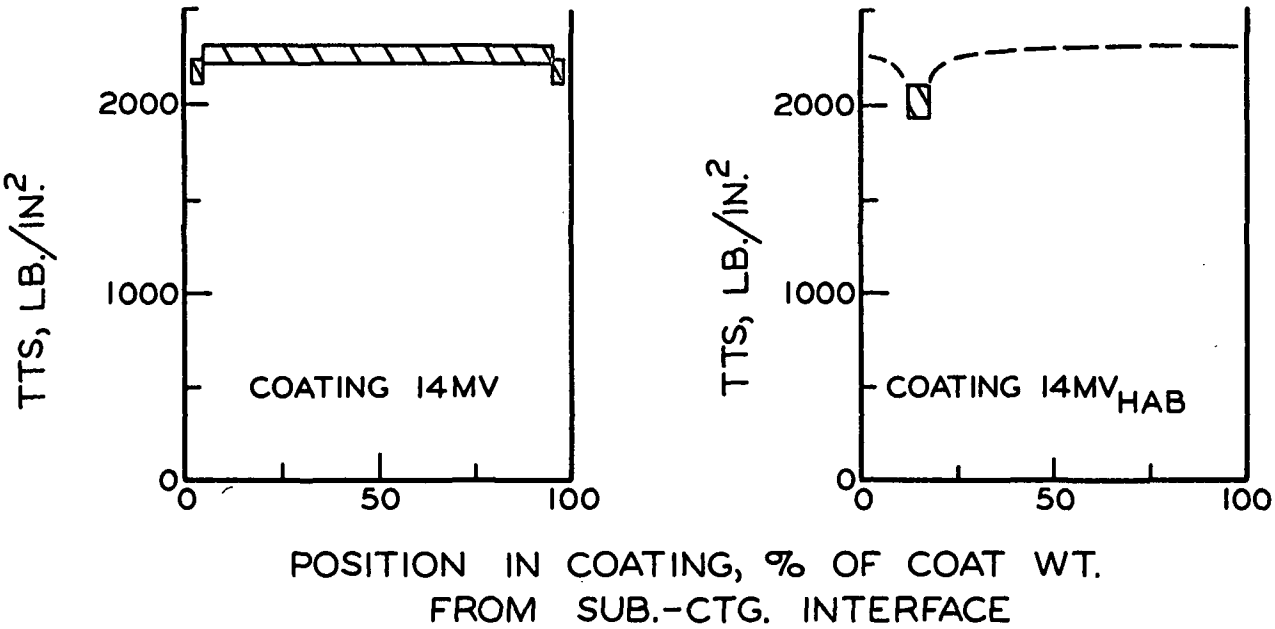

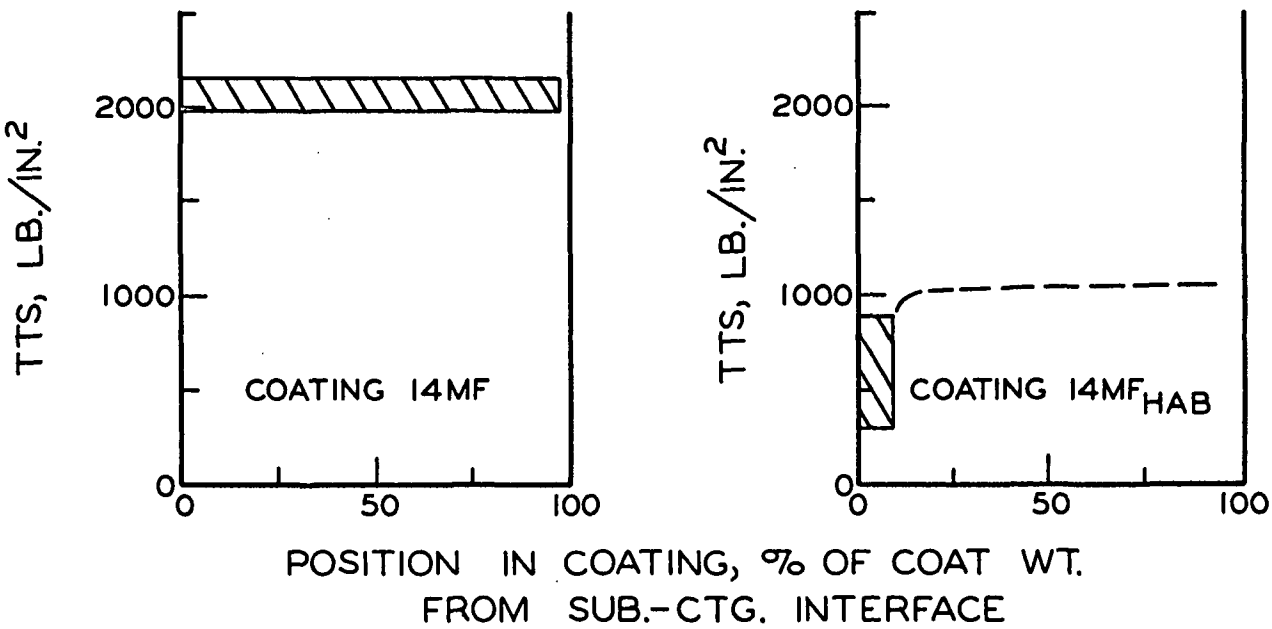

Figure 17. TTS vs. Method of Drying

porous substrate competes with the capillary forces generated by the drying action. Note that the blast-dried coating on "MF", $14MV_{HAB}$ retained significantly more of its original adhesive than the coating on "MF" dried by natural convection at 73°F. The layers near the surface of the coating on "MF" appeared to be strengthened by blast drying, indicating that part or all of the increased starch retention is in the surface layers.

The adhesive distributions given by Dappen (21) for clay-starch coatings on glass and paper dried with a hot air blast show minimum adhesive contents at the same relative locations within the coating as minimum TTS's were found in this study. On nonporous substrates, foil or glass, the minimum adhesive ratio and the zone of weakness in TTS are both adjacent to the substrate. On porous substrates, such as "MF" and paper, the minimum adhesive ratio and the zone of weakness are near the substrate side of the coating. Dappen did not characterize the adhesive distribution in the zone directly adjacent to the paper because of limitations in his method; however, he postulated that this zone might be higher in adhesive concentration than the zone of minimum starch content.

In short, the TTS distributions of these coatings correlate very closely with the known or postulated adhesive distributions for similar coatings.

The physical structure and properties of coatings 14MV and $14MV_{HAB}$ are different. Qualitative evidence of this is that the blast-dried coating is much more brittle. Very little bending is needed to break

the isolated coating. Increased starch concentrations at the two surfaces of the coating could explain such brittleness, since thick films of Stayco M starch are so brittle they shatter like glass. The thinner the film of Stayco M the more flexibility and toughness it seems to have. Additional evidence is provided by the depth of epoxy adhesive penetration. The much lower penetration into $14MV_{HAB}$ suggests that the surface pores are more constricted, probably by starch.

Examination of stained cross sections showed that the depth of starch penetration into the "MF" was less than for coatings dried in air at 73°F. This agrees with the net adhesive ratio data.

Apparent density determinations by the mercury intrusion method indicated that the blast-dried coating had about the same void volume as the one dried in air at 73°F. The slightly lower apparent density of the blast-dried coating could be accounted for by the increased starch retention.

COAT WEIGHT

Until now, no mention has been made of coat weight variations and their effect on TTS. The extent of variation has been indicated for each set of results by giving twice the standard deviation as a measure of dispersion.

Careful examination of the TTS data for coatings on "MF" has revealed no significant effects due to variations in coat weight from 10 to 30 lb./ream. Kraske (17), in his study of coating structure, found coatings of 10, 20, and 30 lb./ream to be nearly identical.

A comparison of coating 12MH at two levels of coat weight is summarized in Table XVI. TTS seems relatively independent of coat weight for the conditions of coating 12MH.

TABLE XVI

TTS VS. COAT WEIGHT FOR COATING 12MH

Coat Weight, lb./ream	Coat Weight Penetrated, lb./ream	TTS, lb./in.^{2}	Location of Failure
13 ± 3	< 1.2	1350 ± 50	Adjacent to substrate
25 ± 11	1	1360 ± 60	Adjacent to substrate

The TTS data for coating 12MF on aluminum foil showed a strong dependence on coat weight; the thin coatings gave much higher strengths than did the thicker ones. Dappen (21) has shown that more starch migrates away from the layer of coating adjacent to the substrate in thicker coatings than in thin ones.

This loss in TTS with increasing coat weight might be found in coatings on porous substrates (1) if the coating is dried very rapidly and/or (2) if the substrate has very small pores.

GENERAL SUMMARY AND THEORETICAL DISCUSSION

As an approach to a more fundamental understanding of the pick strength of pigment-coated papers, it was proposed to study the internal TTS of clay-starch coatings; it was felt that TTS was an important contributing factor in pick strength. Variables affecting coating TTS were reviewed. For a given adhesive and pigment the primary variables in TTS were thought to be:

1. Void volume distribution
2. Stress concentrations
3. Residual stresses
4. Particle alignment
5. Adhesive concentration and distribution

Adhesive distribution was considered an important, if not the controlling, variable.

Secondary variables, affecting TTS indirectly through the primary variables, included:

1. Coating formulation
2. Solids content of coating
3. Method of application
4. Substrate
5. Drying method

Briefly stated, the problem was to evaluate the role of adhesive distribution in determining the TTS of clay-starch coatings. The materials selected for this study included:

1. A hypochlorite-oxidized cornstarch, Stayco M, of low viscosity.
2. A secondary Georgia kaolin available in three particle-size fractions, 0.0-0.5, 0.5-1.0, and 1.0-2.0 mu, e.s.d.
3. A porous substrate (Millipore Filter) soluble in certain organic solvents that do not swell starch and that are available in several well-defined pore sizes; types with 0.10, 0.45, and 0.80 mu pore sizes were used.

The determination of the internal TTS of clay-starch coatings required the development of a new method based on an old principle. The principle is that TTS can be measured by cementing flat, solid surfaces to either side of the specimen and pulling the specimen apart in a tensile tester. Of the several versions of this test in existence, none was satisfactory for testing the internal TTS of clay-starch coatings of commercial thickness. The difficulties, which were overcome by the newly developed method, were mainly (1) undesirable adhesive properties, (2) lack of means for reproducible assembly of the test cylinders and specimen, and (3) lack of means of applying a uniform, simple transverse tensile stress to the specimen.

The adhesive difficulties were overcome with a relatively new adhesive of the epoxy type. The other difficulties were surmounted by designing and building (1) an apparatus for mounting specimens and (2) alignment devices for use in a tensile tester.

Techniques were developed to measure the epoxy adhesive penetration and the location of failure in the coating. The net adhesive ratio was determined by a method based on the starch-iodine color reaction.

The experimental design consisted of holding constant certain factors, such as (1) coating formulation, (2) coating solids content, (3) method of application, (4) adhesive, and (5) type of pigment, and changing in a controlled manner certain variables thought to affect adhesive distribution and TTS. These independent variables were:

1. Pigment particle size
2. Substrate pore size
3. Initial adhesive ratio
4. Method of drying
5. Coat weight

Coatings were prepared with each of the three clay fractions and applied to three substrates, each with a different pore size. Three initial adhesive ratios and two methods of drying were included in the study. All coatings were applied to aluminum foil as well as to the porous "MF". Coat weight was varied from 10 to 30 lb./ream (25x38—500). The results obtained were discussed for each independent variable.

TTS VS. INDEPENDENT VARIABLES

Pigment particle size was found to affect the TTS of coatings on "MF", the smaller the particle size the greater the internal TTS of the coating. Coatings on foil, however, did not show a relationship between TTS and pigment particle size. Pigment particle size appeared to affect TTS by its influence on coating structure and adhesive distribution. Smaller clay particles form a coating with smaller pores, according to Kraske (17), and the smaller the pores the more uniform seems to be the

coating. For a given net adhesive ratio, the smaller the clay particles the thinner must be the layer of starch adjacent to each particle, because small particles have more surface area per gram than large particles. Because thin films of Stayco M are tougher and more flexible than thick films, the coating whose adhesive is distributed as thin films may be stronger than one with thicker adhesive films, for a given adhesive concentration.

The apparent density of the coatings decreases when particles become larger and less easy to fit into a compact structure; for a given adhesive ratio, the volumetric starch concentration tends to decrease as pigment particle size increases.

Substrates with small pores were found to withdraw larger amounts of starch from the coating and to produce weaker coatings than substrates with large pores.

Pigment particle size and substrate pore size produced an interaction effect when the clay particles were smaller than the substrate pores. The resulting coating had a narrow zone of weakness near the air surface of the coating which was not found in the other coatings. Such coatings set rapidly and, it is thought, assume a more random particle orientation than similar coatings in which the pigment does not penetrate the substrate. The weak zone appears to result from the competition for the vehicle between the porous substrate and the drying surface. Adhesive migrates with the vehicle in both directions from the weak zone leaving a layer of coating depleted in starch.

For coatings both on "MF" and on foil TTS increases with increasing initial adhesive ratio. The net adhesive ratio also increases with increasing initial adhesive ratio. The coating on "MF" at the lowest adhesive ratio had a broad zone of weakness in the upper half of the coating, whereas similar coatings at higher adhesive ratios were more uniform in strength. This suggests that adhesive migration is more pronounced at lower starch concentrations.

Drying affected coating TTS very markedly. Hot air-blast-dried coatings retained more starch but had a zone of weakness near the substrate with lower TTS than coatings dried more slowly. Increased adhesive migration due to drying seems to explain the results adequately. The blast-dried coating was more brittle, probably due to an increased starch concentration near the air surface.

Coat weight had little effect on the TTS of coatings on "MF", but in one coating on foil TTS showed a strong dependence on coat weight. It is believed that this effect was due to greater adhesive migration in the thicker coatings, resulting in a weaker, starch-depleted layer near the foil.

TTS VS. PRIMARY VARIABLES

The influence of the above independent variables on the internal TTS of clay-starch coatings has been explained in terms of variables previously classified as primary to TTS. These primary variables are:

1. Void volume distribution
2. Stress concentrations

3. Residual stresses

4. Particle alignment

5. Adhesive concentration and distribution

The results of this study made possible a clearer understanding of the roles played by the above variables in the internal TTS of pigment coatings. The following discussion, based on the coatings studied, is advanced with due regard to the limitations of the experimental design. Interpretations are thus qualitative and not necessarily complete or conclusive.

Voids or pores may be considered a secondary factor in the TTS of pigment coatings, because they affect TTS through other variables such as stress concentrations and adhesive distribution. The configurations and distribution of pores are probably determined by particle alignment and adhesive redistribution. A knowledge of the pore structure of a coating is desirable in order to describe the volumetric distribution of the adhesive. The adhesive ratio and coat weight data describe the distribution of adhesive in two dimensions, i.e., in the plane of the coating. In the third dimension, perpendicular to the coating, the average adhesive concentration can be calculated if the apparent density of the coating is also known.

The results of this and other studies have supplied considerable evidence showing that coating behavior is profoundly affected by transverse variations within the coating, particularly with respect to transverse variations of the adhesive concentration. Average adhesive concentration must be replaced by volumetric or three-dimensional

adhesive distribution. Not only the volume distribution of adhesive but also its configurations are important in coating strength. The void volume distribution helps describe the adhesive configurations, for example, whether the adhesive is distributed as thick films or membranes with large voids or as thinner films more closely knit together. Pigment particle size may also be important in determining the adhesive configuration.

Stress concentration and large voids may be caused by adhesive redistribution and help explain the apparently close relationship between TTS and the final adhesive distribution. Stress concentrations in pigment coatings have not been measured, probably because of experimental difficulties; but the presence of stress concentrations can be postulated from work on other systems. When the coating is subjected to stresses, the nonuniform adhesive distribution and the heterogeneity of the coating promote variations in strain from point to point, giving rise to stress concentrations. The greater the heterogeneity, the greater and more influential are the stress concentrations.

Residual stresses may likewise be considered a product of adhesive distribution because it is principally the adhesive that creates residual stresses during drying. On drying, a thick film of starch will curl into a rigid, distorted shape, whereas a thin film will tend to dry flat. The distortion of the thick film is accompanied by residual stresses, and the film shatters on slight impact. In clay-starch coatings uneven drying tends to cause brittleness as well as nonuniform starch

distribution. Even with a uniform adhesive distribution, the starch may develop residual stresses as it shrinks within a semirigid clay structure.

Particle alignment, like voids, appears to influence TTS through its effect on the structural distribution of the starch. Hemstock and Swanson (4) suggested that for coatings on foil very perfect particle alignment adjacent to the foil surface resulted in a strong void-free coating. Results of the present study show that (1) coatings on foil are not stronger in TTS than coatings on porous substrates and (2) failure in TTS occurs in layers where particle orientation should be a maximum, for example, adjacent to smooth substrates.

The role of particle alignment in TTS definitely seems of minor importance in comparison to that of adhesive distribution. Since surface stresses caused by bending are less for thin coatings than for thick coatings, particle alignment may influence coating behavior involving bending by a reduction in the thickness per unit weight of coating. The final distribution of the adhesive within the coating emerges as the most significant variable in determining the internal TTS of clay-starch coatings. The final starch distribution in the coating, as it is presently understood, can serve as a basis for explaining all of the TTS results obtained in this study. Factors favoring a starch configuration strong in TTS are:

1. A uniform volumetric distribution of starch throughout the coating
2. Small pores or voids uniformly distributed within the coating
3. Small pigment particles randomly oriented

4. High volumetric starch concentrations

The penetration of starch into the substrate and rapid drying both tend to reduce TTS by creating zones of low volumetric starch concentration.

CONCEPT OF ADHESIVE DISTRIBUTION

Because of the noticeable connection between TTS and adhesive distribution, it is worthwhile to consider how the final adhesive distribution may be created. The following concept of adhesive distribution is based on the limited study described above and must be regarded as tentative.

The key point of this concept is to visualize the coating and the substrate as competing capillary systems. The competition exists over the liquid vehicle which, incidentally, tends to transport starch when it migrates. The capillary system of "MF", unlike paper, is well-defined and does not change when an aqueous coating is applied. The capillary system of the coating is nonexistent until the particles coalesce or set in a coherent structure. As the vehicle is withdrawn from the layer of coating adjacent to the substrate, the pigment particles in that layer are brought closer together until they are immobilized. The interparticle voids of this immobilized layer serve as capillaries through which the vehicle from upper layers must pass to reach the substrate.

Neglecting vehicle migration due to drying and making several rather gross assumptions, one can compare the rate of flow of the vehicle in the "set" coating layers with the rate of flow into the substrate assuming

the two rates to be independent of each other. Since the two rates must in fact be equal, the smaller rate will tend to determine the actual flow rate.

For the substrate it has been shown above that

$$\underline{dL/dt} = 1/2\ (\underline{r_s}\gamma \cos\theta)^{1/2} / (2\eta\,\underline{t})^{1/2} \qquad (6)$$

To express penetration on a volume basis:

$$\underline{dV/dt} = \underline{k_1 A}\ \underline{dL/dt} = \underline{k_1 A}\ (1/2)(\underline{r_s}\gamma \cos\theta)^{1/2} / (2\eta\,\underline{t})^{1/2} \qquad (7)$$

where $\underline{k_1}$ = void fraction of the substrate (about 0.8 for "MF")

$\underline{A}$ = area to which coating is applied, $cm.^2$ ($1\ cm.^2$ is taken as a basis)

Applying Poiseuille's law for laminar flow in a capillary to the coating:

$$\underline{dV/dt} = (\underline{k_2 A r_c \Delta P})/(8\eta\,\underline{L_c}) \qquad (8)$$

where $\underline{k_2}$ = void fraction of "set" coating [about 0.5, based on % voids_{H_2O} data of Cobb (40)]

$\underline{r_c}$ = volume average pore radius of "set" coating, cm.

$\underline{\Delta P}$ = driving pressure, $g./cm.^2$

$\underline{L_c}$ = length of capillaries, cm.

$$\underline{\Delta P} = (2\gamma \cos\theta)/(\underline{r_s}), \text{ neglecting effects of gravity and cavitation} \qquad (9)$$

$$\underline{L_c} = (\underline{L_f}/\underline{V_t})(\underline{V}) \qquad (10)$$

where $\underline{L_f}$ = thickness of total "set" coating, cm.

$\underline{V_t}$ = total volume of vehicle that must be withdrawn from coating to cause setting, $cm.^3$

Substituting Equations 9 and 10 into 8:

$$\underline{dV}/\underline{dt} = (\underline{k_2}\underline{Ar_c}^2\gamma \cos\theta)/[4\eta\, \underline{r_s}(\underline{L_f}/\underline{V_t})\underline{V}] = \underline{K}/\underline{V} \qquad (11)$$

Integrating from $\underline{V} = 0$ to $\underline{V} = \underline{V}$ and $\underline{t} = 0$ to $\underline{t} = \underline{t}$:

$$\underline{V}^2/2 = \underline{Kt} \qquad (12)$$

$$\underline{V} = (2\underline{Kt})^{1/2} \qquad (13)$$

Substituting Equation 13 into 11 to eliminate $\underline{V}$:

$$\underline{dV}/\underline{dt} = (\underline{k_2}\underline{Ar_c}^2\gamma \cos\theta)^{1/2}/[8\eta\, \underline{r_s}(\underline{L_f}/\underline{V_t})\underline{t}]^{1/2} \qquad (14)$$

Comparing Equations 6 and 14:

Coating

$$\underline{dV}/\underline{dt} = (\underline{k_2}\underline{Ar_c}^2\gamma \cos\theta)^{1/2}/[8\eta \underline{r_s}(\underline{L_f}/\underline{V_t})]^{1/2}$$

Substrate

$$\underline{dV}/\underline{dt} = \underline{k_1}\underline{A}(1/2)(\underline{r_s}\gamma \cos\theta)^{1/2}/(2\eta\underline{t})^{1/2}$$

Cancelling terms, the controlling flow rate will depend on whether or not $(\underline{k_2}\underline{r_c}^2)/[(\underline{L_f}/\underline{V_t})\underline{r_s}]$ for the coating is greater than $(\underline{k_1}\underline{Ar_s})$ for the substrate.

For the large clay fraction on the small pore size substrate, i.e., coating 12LV:

$\underline{k_2} = 0.5$

$\underline{L_f}/\underline{V_t} = 1.65$ cm./cm.^{3} (calculated from % voids_{H_2O} data of Cobb (40) for a coat weight of 20 lb./ream and initial coating solids of 55%)

$\underline{k_1} = 0.8$

$\underline{A} = 1$ cm.^{2}

$\underline{r_c} = 0.08$ mu [volume average pore size of coating with large clay fraction on "MF", type HA, obtained by Kraske (17)]

$\underline{r_s} = 0.05$ mu

Therefore, $(k_2 r_c^2)/[(L_f/V_t)r_s] = 4 \times 10^{-6}$ for the coating, and $k_1 A r_s = 4 \times 10^{-6}$ for the substrate.

In this case the substrate seems to provide as much restriction to the flow as does the coating. For the other pigment-substrate combinations in this study the coating should be rate-controlling, because r_s is larger and r_c smaller than for the above example.

The above comparison is extemely qualitative. Some of the objections that could be raised are:

1. The driving pressure due to the vehicle wetting the substrate pores must be shared by the coating and the substrate. It was assumed above that the coating and substrate each had the total driving pressure acting on it. As a partial justification of the assumption it should be pointed out that the component having the greater flow restriction will consume a larger portion of the driving pressure than the other component will.

2. The pores were assumed to be straight, cylindrical capillaries of uniform radii. A comparison of Equation 8 with the Kozeny-Carman equation for viscous flow in granular beds was made. For a void fraction of 0.57, Kozeny-Carman constant of 5, and a particle specific surface of 3×10^5 cm.^{2}/cm.^{3}, as obtained by Grace (41) for kaolin dispersed with 0.1M $Na_4P_2O_7$, the two equations gave flow rates agreeing within 15%. Since the Kozeny-Carman constant, K, makes no assumptions as to path length or tortuosity, the assumption of straight, cylindrical capillaries of uniform radii does not appear to introduce a large error.

The value for the radii of coating pores was obtained on dried coating. Probably the effective radius of the pores in the first layer of coating to flocculate is much greater than is found in the dried coating. The adhesive may tend to reduce the effective pore radius if it is selectively adsorbed or otherwise held by the pigment. Dintenfass (42) has shown that China clay adsorbs polar groups in the following decreasing order: (1) primary amine, (2) secondary amine, (3) hydroxyl, and (4) carboxyl. Therefore, casein and gelatin would tend to be adsorbed more than starch and restrict vehicle flow to a greater extent.

In the substrate the pore radius is reduced if adhesive collects along the walls of the pores.

3. The viscosity was assumed constant for the vehicle flowing both in the coating and in the substrate. It would seem that the vehicle viscosity would be greatest at the upper surface of the coating and decrease because of loss of adhesive as the vehicle penetrates into the substrate. Dappen (21) showed that much more water than starch leaves the coating due to bodystock penetration. The effect of decreasing vehicle viscosity may tend to compensate for the reduction in pore size as the adhesive builds up in the passages of the coating.

4. The volume of vehicle that must be withdrawn from the coating to cause setting, V_t, was calculated from data on a clay slip having no adhesive. In the presence of adhesive, V_t should be less than for

water alone and may also be a function of the rate of vehicle loss from the coating, because coatings losing vehicle more rapidly seem to set in a looser, more random particle arrangement.

5. For substrate pores smaller than 1 mu in radius the driving pressure is theoretically greater than atmospheric pressure. If cavitation limits the driving pressure to a value near 14.7 lb./in.^{2}, the rate of penetration induced by pores smaller than 1 mu radius should be directly proportional to the pore radius, rather than to the square root of the pore radius. The comparison of flow rates would then be:

$(k_2 r_c^2)/(L_f/V_t)$ for the coating

$(k_1 A r_s^2)$ for the substrate

The flow rate in the coating is now independent of the substrate pore size. Relative flow rates for the clay fractions and substrates used in this study are given in Table XVII.

TABLE XVII

VEHICLE FLOW RATES VS. PIGMENT PARTICLE SIZE AND SUBSTRATE PORE SIZE

Clay	Pore Radius,[a] mu	Relative Flow Rate[b]	"MF" Type	Pore Radius, mu	Relative Flow Rate
S	0.039	22	VC	0.050	14
M	0.054	31	HA	0.225	64
L	0.079	46	AA	0.40	113

[a] Volume average pore radius in dried coating, as given by Kraske (17).

[b] In arbitrary units; the values given are only for comparisons within this table.

The above comparison at a constant driving pressure of one atmosphere indicates that "MF", type VC, will limit the rate of vehicle penetration of coatings made with any of the three clay fractions in this study. The coating should control penetration rate on the other two types of "MF". If coatings on "MF", type VC, can supply vehicle faster than the substrate can absorb it, this may help explain why so much more adhesive is able to migrate with the vehicle for coatings on VC than on HA or AA.

Assuming that the penetration rate is controlled by the substrate and using the % $voids_{H_2O}$ data of Cobb (40) to determine the volume of vehicle that must be removed from the coating for it to set, one can calculate the approximate setting times required by coatings 12MV and 12MA. The calculation, given in Appendix VII, shows that 12MV should require 24 seconds and 12MA three seconds. These values are in approximate agreement with the experimentally observed setting times for these coatings. This does not prove the validity of the concepts presented, but it does suggest that the setting times of coatings may provide significant information about the coating-substrate relationship.

The use of pigment volume concentration, as emphasized by Cobb (40), seems to be a valuable step forward. The contribution of pigment voids to adhesive distribution appears to depend on:

1. Viscosity of the migrating vehicle
2. Size and configurations of interparticle channels available for vehicle migration.

The vehicle viscosity is a function of the adhesive ratio, the per cent solids of the coating, the type of adhesive, and the degree of adhesive adsorption on the pigment. The size and configuration of interparticle flow channels depends on such factors as pigment particle size and shape, adsorption of adhesive on pigment, particle alignment, nature of pigment surface, and rate of flow of the vehicle.

It would seem useful to determine the per cent voids of the pigment with the vehicle to be used in the coating rather than with water. The effects of adhesive and adhesive concentration would thus be included. The results should be useful in predicting the rate at which a given coating will set.

Once the coating has set, a framework is established within which the vehicle must move to redistribute the adhesive. But even before the coating sets, the forces caused by drying are tending to increase the adhesive concentration at the air surface of the coating. If penetration is slow and the drying rate is small, the coating is likely to have a nearly uniform starch distribution but may lose a large fraction of its original starch content.

On the other hand, if drying is rapid and the rate of vehicle penetration is large, the coating may have a zone of low adhesive content; but most of the original adhesive will probably be retained within the coating.

The "water-retention tests" described by Frost (43) and by Stinchfield, Clift, and Thomas (44) seem to be a relative measure

of the capillary structure created in the coating by the loss of vehicle; therefore, they are of theoretical as well as practical interest to coating technologists. In addition, the volume of vehicle that must be removed to set a given volume of coating probably has a strong effect on the water-retention test. The contribution of the latter factor to water retention could be evaluated by determining the % voids of the pigment with coating vehicle instead of water.

The results of the present study have suggested an alternate explanation of the immobilization data obtained by Hemstock and Swanson (45). The decreasing volume of vehicle migrating ($\underline{I}$) as the solids content of clay slips is increased, was attributed to the efficiency of clay particles plugging the pores in the paper bodystock. An alternate explanation is that (1) at higher solids there is less water available per unit volume of clay slip and (2) the interparticle channels are smaller, tending to reduce the rate of flow. The increase in $\underline{I}$ after passing through a minimum could be due to an inherent limitation in the method of determining $\underline{I}$, rather than to an actual increase in $\underline{I}$. A factor causing an increase in the thickness of clay or coating left on the paper wound around the roll causes an apparent increase in $\underline{I}$. At higher solids the clay may be immobilized by flocculation in a loose structure with only a small loss of water to the paper, the rest of the water being in the voids between clay particles. This situation is similar to the phenomenon of dilatancy.

The large difference in $\underline{I}$ between sucrose solutions and clay slips was attributed to particle plugging. It is suggested that the

resistance to flow within the clay slip because of the formation of a capillary structure could explain the lower $\underline{I}$ in the case of clay slips.

TTS AND PICK STRENGTH

A major contribution of an understanding of the TTS of clay-starch coatings lies in relating this understanding to coating strength in general and to pick strength in particular.

This study of TTS has touched on many facets of coating strength; but until the components of coating strength which are involved in pick strength are more clearly defined, it is almost impossible to make any definite correlations between TTS and pick strength. It must be borne in mind that pick strength usually involves coatings on paper, whereas this study was concerned with the internal TTS of coatings applied, not to paper, but to "MF". "MF" differs from paper in at least five ways:

1. "MF" has pores of very uniform size.
2. Pores in "MF" are oriented perpendicular to the sheet.
3. "MF" has a very high void fraction, about 80% of the total sheet volume.
4. The surface of "MF" is much smoother than the usual paper bodystock.
5. "MF" does not swell when an aqueous coating is applied to it.

However, certain observations have been made during this work which bear on pick strength.

The difference between TTS and pick strength can be illustrated by two examples:

1. Clay-starch coatings have much greater TTS than the typical paper bodystock, yet failure by picking may occur within the coating.
2. The pick strength of a clay-starch coating depends on the substrate, even though failure occurs in the coating. Coatings on aluminum foil had much greater pick strength than the same applied to porous substrates such as paper or "MF", yet the coatings on foil had about the same TTS as the coating on "MF".

Since the substrate is so important in pick strength, the distribution of adhesive penetrating the substrate is significant. It was observed that for low rates of penetration the starch remained in a narrow zone of the substrate directly adjacent to the coating. At higher rates of penetration less starch was lost from the coating, but it was distributed over a thicker zone of the substrate than in the case of the lower penetration rate. If reinforcement of the surface layers of the substrate plays an important role in pick strength, low rates of vehicle penetration seem desirable, other factors being equal.

At low adhesive ratios the zone of failure in the picking of casein-clay coatings on paper usually occurred in the coating about a micron away from the bodystock, according to Singleterry (21). A thin layer of clay particles was observed remaining on the fibers. The explanation advanced was that the adhesive concentration passed through a minimum at the zone of failure and then increased to a higher value at the bodystock-coating interface. A consideration of the coating

immediately after application suggests that the vehicle will leave the coating primarily by flowing between fibers rather than through or into them. In viscous flow the liquid near stationary surfaces travels more slowly than the liquid in the center of the channel. Thus, the layer of coating near the surface of a fiber will tend to be immobilized while flow proceeds around the fiber from points farther away from the fiber surface. After the coating has set, flow of vehicle would still tend to be greater in the center of interfiber or interparticle pores rather than at the fiber-coating interface. A tendency for clay platelets to orient parallel to the fiber surface would increase the immobilization of pigment particles on the fibers.

For the coating bridging the interfiber spaces, the adhesive distribution should be analogous to that of the coatings described in this study; and the zone of weakness might be directly at the coating-bodystock interface in some coatings, and farther away from the interface in others.

During the experimental work it was observed that some coatings were more brittle than others but that this brittleness did not seem to affect TTS. The hot air-blast dried coating on "MF", for example, was quite brittle and fractured under slight bending; yet its TTS was much higher than other, more flexible coatings. Such brittleness would probably be extremely detrimental to pick strength. Coatings with lower apparent densities are likewise unable to resist as much bending, because of the greater stresses created at their surfaces, as can denser coatings of equal coat weight.

CONCLUSIONS

The following conclusions are based on this study of the internal TTS of clay-starch coatings:

1. A method and an apparatus have been developed for measuring the internal TTS of clay-starch coatings.
2. Techniques have been developed for determining the total depth of epoxy adhesive penetration and the location of failure in clay-starch coatings tested by the new TTS method.
3. The TTS of the clay-starch coatings isolated from "MF" with ethyl acetate is relatively insensitive to conditioning at different relative humidities and to the rate of loading used in the testing.
4. Other factors being equal, a coating applied to a substrate with small pores loses more adhesive to the substrate and has less TTS than does the same coating applied to a substrate with larger pores.
5. Other factors being equal, coatings made with larger clay particles and applied to a porous substrate have less TTS than coatings with smaller clay particles.
6. On a nonporous substrate the TTS of a coating is not directly related to pigment particle size.
7. The TTS of clay-starch coatings increases with increasing adhesive concentration.
8. When applied to a porous substrate, coatings dried with a hot-air blast retain more adhesive but have less TTS than coatings dried by natural convection at room temperature.

9. When applied to a nonporous substrate, coatings dried with a hot-air blast have less TTS and fail nearer the substrate than coatings dried by natural convection at room temperature.

10. Variations in coat weight have little effect on the TTS of clay-starch coatings on porous substrates such as "MF".

11. On nonporous substrates, thick coatings tend to be weaker in TTS than thin coatings, and the failure occurs near the substrate instead of randomly.

12. The amount of starch lost from a coating is not necessarily related to the depth of penetration of starch into the substrate.

13. Greater particle orientation does not necessarily increase TTS.

14. The TTS of clay-starch coatings seems to be largely governed by the final adhesive distribution in the coating. The distribution of voids and degree of particle orientation apparently affect TTS through their effects on the adhesive distribution.

SUGGESTIONS FOR FURTHER RESEARCH

To further the understanding of coating strength in general and pick strength in particular, the following paths of investigation are suggested:

1. A study of the variables affecting the shear and flexural strengths of pigment coatings;
2. A study of various adhesive-pigment combinations with respect to TTS and adhesive distribution;
3. A study of coating strength and adhesive distribution as a function of "water retention";
4. A study of adhesive distribution and coating strength as a function of various means of drying, e.g., hot surface, dielectric, and high-velocity air jet drying methods;
5. An analytical study of coating strength as a function of the volumetric adhesive distribution within pigment coatings.

ACKNOWLEDGEMENT

The assistance and constructive criticism of Mr. Henry W. Marx in the design and construction of "the apparatus for mounting specimens for the evaluation of TTS" is gratefully acknowledged.

LITERATURE CITED

1. Wink, W. A., Clinton, T. J., Thickens, R. W., and Van den Akker, J. A., Tappi 35, no. 9:181-8A(Sept., 1952).

2. Wink, W. A., Shillcox, W. M., and Van Eperen, R. H., Tappi 40, no. 7:189-99A(July, 1957).

3. Blokhuis, G., Lenaarts, W., Lodewijks, L. J., and Monroy, J. F. The printability of paper. Manual of the I.G.T. printability tester. No. 12. 2nd ed. Amsterdam, Holland, Institute for the Graphic and Allied Industries, May, 1955.

4. Hemstock, G. A., and Swanson, J. W., Tappi 40, no. 10:794-801 (Oct., 1957).

5. Wheeler, G. C., Tappi 38, no. 2:132-4A(Feb., 1955).

6. Casey, J. P. In Pulp and paper, chemistry and chemical technology. Vol. 2. p. 1107. New York, Interscience, 1952.

7. Barber, E. J., and Davis, J. W., Tappi 34, no. 10:433-8(Oct., 1951).

8. King, C. F., Inland Printer 126, no. 1:79-82(Oct., 1950).

9. Roehr, W. W., Tappi 34, no. 11:525-8(Nov., 1951).

10. Savage, R. H., Tech. Assoc. Papers 11, no. 1:237(1928).

11. Casey, J. P. In Pulp and paper, chemistry and chemical technology. Vol. 2. p. 1104. New York, Interscience, 1952.

12. Annis, H. M., Tech. Assoc. Papers 19:46-7(1936).

13. Kirkpatrick, W. A., II, Tech. Assoc. Papers 22, no. 1:322-4; discussion, 113-6(June, 1939); Paper Trade J. 109, no. 12:36-8 (Sept. 21, 1939).

14. Arnamo, A., Olsson, I., and Pihl, L., Svensk Papperstidn. 55, no. 18:709-14(Sept. 30, 1952).

15. Bekk, J., Paper-Maker 89, no. 6:TS88-9(June 1, 1935); Paper Makers' Assoc. Gt. Brit. & Ireland Proc. Tech. Sect., 16, part 1:30-2(Oct., 1935).

16. The Staff of The Institute of Paper Chemistry. Determination of the bonding strength of paper. Part I. Report No. 31 to The American Paper and Pulp Association, Instrumentation Program. Appleton, Wis., The Institute of Paper Chemistry, Feb. 3, 1941.

17. Kraske, D. J., Methods for the evaluation of the physical structure of clay-starch coating films. Doctor's Dissertation. Appleton, Wis., The Institute of Paper Chemistry, 1959. 156 p.

18. Roderick, H. F., and Hughes, A. E., Tech. Assoc. Papers 23:287-91 (1940).

19. Hughes, A. E., and Roderick, H. F., Tech. Assoc. Papers 23:610-15 (1940).

20. Singleterry, C. R., Paper Trade J. 113, no. 18:37-40(T.S. 233-6) (Oct. 30, 1941); Tech. Assoc. Papers 25:641-4(1942).

21. Dappen, J. W., Tappi 34, no. 7:324-35(July, 1951).

22. Dreshfield, A. C., Jr., and Han, S. T., Tappi 39, no. 7:449-55 (July, 1956).

23. Kesler, C. C., and Bechtel, W. G., Anal. Chem. 19, no. 1:16-21 (Jan., 1947).

24. Millipore Filter Corporation. Millipore Filters. Watertown, Mass., Millipore Filter Corp., 1957. 16 p.

25. Paper Makers' Mo. J. 61, no. 12:495(Dec. 15, 1923); Biblio. Series 139-44, no. 118:33. Appleton, Wis., The Institute of Paper Chemistry, June, 1949.

26. Abrams, A., Paper Trade J. 91, no. 4:56(July 24, 1930); Tech. Assoc. Papers 13:39(1930).

27. Kessler, J. R., Tech. Assoc. Papers 10:232(1927).

28. Sutermeister, E., and Porter, L. W., Paper Trade J. 90, no. 12:73-4 (Mar. 20, 1930); Tech. Assoc. Papers 13:206-7(1930).

29. Brecht, W., and Klikstad, F., Papier-Fabr. 38, no. 8:50-1(Feb. 23, 1940).

30. Sutermeister, E., and Osgood, H. W., Jr., Tech. Assoc. Papers 24:136-8(1941).

31. The Staff of The Institute of Paper Chemistry, Paper Trade J. 123, no. 18:24, 26, 28-9; no. 19:24, 26, 28, 30, 32, 34(Oct. 31, Nov. 7, 1946).

32. Wink, W. A., and Sears, G. R., Tappi 33, no. 9:96-9A(Sept., 1950).

33. McHenry, D., and Shideler, J. J. In ASTM Special Tech. Bull. no. 185. p. 74. Philadelphia, Pa., ASTM, July, 1956.

34. Dietz, A. G. H., and McGarry, F. J. In ASTM Special Tech. Bull. no. 185. p. 40. Philadelphia, Pa., ASTM, July, 1956.

35. Ritland, H. N. In ASTM Special Tech. Bull. no. 185. p. 24. Philadelphia, Pa., ASTM, July, 1956.

36. Browning, B. L., Bublitz, L. O., and Baker, P. S., Tappi 35, no. 9:419-20(Sept., 1952).

37. Washburn, E. W., Phys. Rev. 17:374-5(1921); C.A. 16:3562.

38. Casey, J. P., and Libby, C. E., Paper Trade J. 127, no. 25:522-9; no. 26:530-6(Dec. 16, 23, 1948); Tech. Assoc. Papers 31:172-85 (1948).

39. Kraske, D. J. Unpublished work, 1958.

40. Cobb, R. M. K., Tappi 41, no. 10:581-600(Oct., 1958).

41. Grace, H. P., Chem. Eng. Progr. 49, no. 6:303-18(June, 1953).

42. Dintenfass, L., Kolloid-Z. 155, no. 2:121-31(Dec., 1957).

43. Frost, F. H., Tappi 35, no. 7:16A, 18A, 20A, 22A(July, 1952).

44. Stinchfield, J. C., Clift, R. A., and Thomas, J. J., Tappi 41, no. 2:77-9(Feb., 1958).

45. Hemstock, G. A., and Swanson, J. W., Tappi 40, no. 10:833-8(Oct., 1957).

APPENDIX I

THE ACTION OF THE IPC BONDING STRENGTH TESTER
WITH A COATING ON A COMPRESSIBLE SUBSTRATE

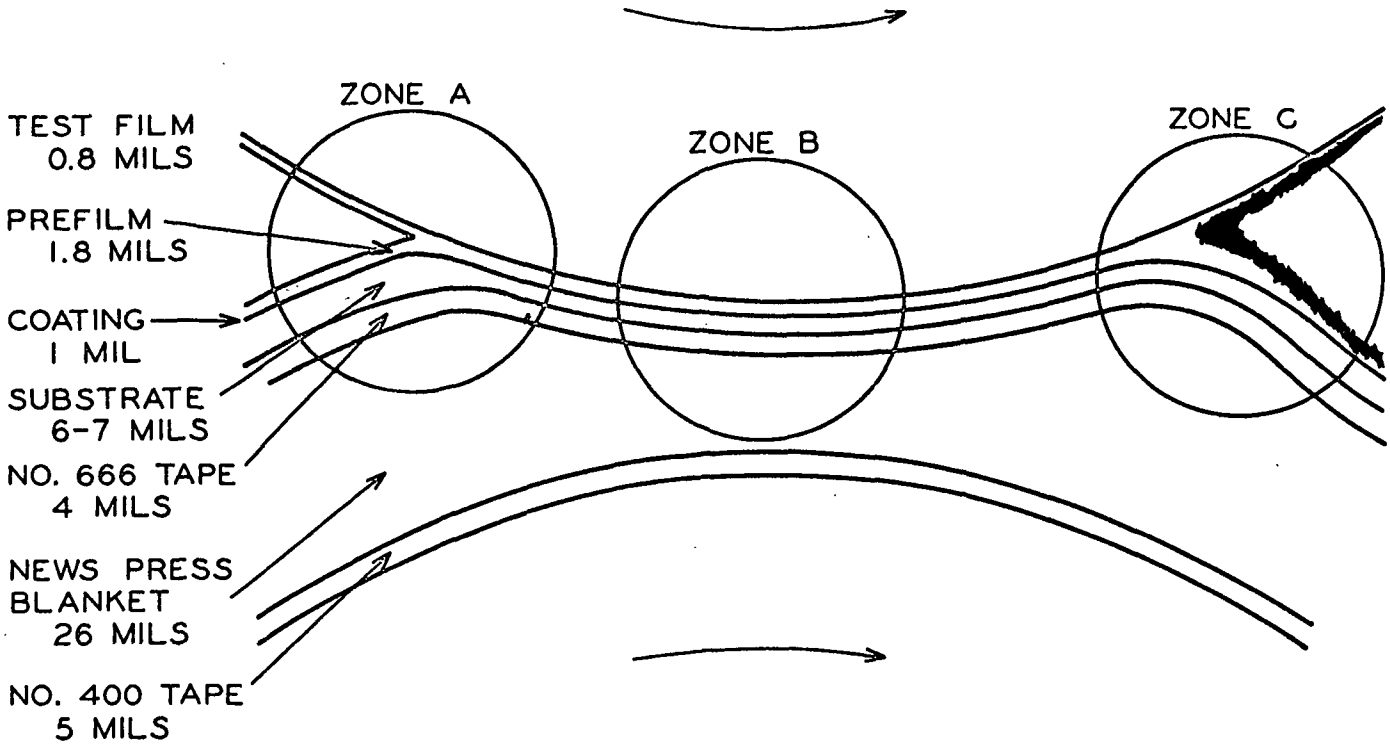

STRESSES IN THE IPC BONDING STRENGTH TEST
OF A COATING ON A COMPRESSIBLE SUBSTRATE

Nature of Stress	Orientation of Stress Relative to Plane of Coating	Location of Stress zones
Tensile	Parallel	B, C
Tensile	Transverse	C
Bending	Transverse	A, C
Compressive	Parallel	A
Compressive	Transverse	B
Shear	Parallel	A, B, C

APPENDIX II

PARTICLE SEDIMENTATION CALCULATION

Because of the large difference in the densities of the pigment and the coating vehicle any action that increases the gravitational forces on the coating will tend to cause stratification of the pigment. A coating roll at high speed will "centrifuge" the pigment away from the roll surface. The importance of this effect can be estimated by Stokes's law.

Frictional drag = gravitational force

$$6\pi\eta\, \underline{r}\underline{u} = (4/3)\pi \underline{r}^3(\rho-\rho')(\underline{v}^2/\underline{r}_o)$$

(transposing)

$$\underline{u} = (2/9)(\underline{r}^2/\eta\ )(\rho-\rho')(\underline{v}^2/\underline{r}_o)$$

where $\underline{u}$ = initial sedimentation velocity, ft./sec.

ρ = density of particle, lb./ft.^{3}

η = viscosity of medium, lb./ft. sec.

ρ' = density of medium, lb./ft.^{3}

$\underline{v}$ = linear velocity of roll surface, ft./sec.

$\underline{r}$ = particle radius, ft.

$\underline{r}_o$ = coating roll radius, ft.

For a suspension of clay particles (0.5 mu, e.s.d.) in water being applied at 1800 ft./min. (surface speed of roll) by a roll 1 ft. in diameter:

$$\underline{u} = (2/9)(8.2\text{x}10^{-7})^2(100)(30)^2/(0.672\text{x}10^{-3}\text{x}1/2)$$

$$\underline{u} = 2.0 \text{ mu/sec.}$$

If the clay suspension travels half way around the applicator roll, the particle displacement, $\underline{x}$, is

$$\underline{x} = (2.0\pi)/(60) = 0.10 \text{ mu}$$

APPENDIX III

PROCEDURE FOR TTS TEST

1. Prepare isolated coating specimens:
   a. Cut 18-mm. diameter disks.
   b. Weigh disks to determine coat weight.
   c. Orient disks on specimen support plate with the original air surface of the coating away from the plate.
2. Clean the ends of the test cylinders with crocus cloth and place them in the specimen mounting apparatus for the evaluation of TTS.
3. Secure test cylinders to the top half of the apparatus with cap screws.
4. Prepare adhesive by adding activator; note time of mixing.
5. Doctor the adhesive on the ends of the test cylinders; remove the excess adhesive from the surfaces of the apparatus with a razor blade. Smear some of the adhesive on a glass plate to test the rate of curing.
6. When adhesive cure has proceeded to the desired extent (tacky but rather firm), place the plate with the specimens in the apparatus; assemble the apparatus.
7. Place apparatus in vacuum desiccator.
8. Evacuate desiccator to 8 cm. Hg absolute pressure with Megavac vacuum pump (2 min. required).
9. Clamp specimens by tightening the nut on the apparatus to the desired pressure; close stopcock at desiccator and shut off vacuum pump.

10. Allow adhesive to cure at room temperature for about half an hour; relieve the vacuum by opening the stopcock at the desiccator.

11. Place apparatus in oven at 74°C. to cure for 2 hours.

12. Remove apparatus from oven; cool to room temperature.

13. Disassemble apparatus and remove test cylinders, using ejector.

14. Trim the edges of the specimen and the adhesive flush with the test cylinders.

15. Mount the test cylinders on the aligning devices in the tensile tester (Baldwin-Southwark or Instron); test at a load rate of 500 lb./min.

16. Record breaking load.

17. Examine fracture with dissecting microscope to see where failure occurred.

18. Quantitatively remove the coating from the test cylinders with a camel's hair brush and water, collecting the coating in a tared beaker; dry coating and weigh beaker to determine the depth of adhesive penetration and the location of failure in the coating.

19. Remove burr of adhesive from the holes in the mounting apparatus with a reamer.

APPENDIX IV

TTS DATA

TABLE I

TTS VS. RELATIVE HUMIDITY CONDITIONING

Coating 12MA[a]

Coat weight = 20±5 lb./ream

Relative humidity, %	11	52	86
TTS, lb./in.^{2}	2100	2140	2430
	2278	2318	2243
	2294	2103	2168
	2390	2245	1993
ave.	2266	2203	2208
σ_m[b]	60	51	90

over-all av. = 2225 lb./in.^{2}

[a] The meaning of the coating symbols is given in the Glossary, p. 23.

[b] σ_m = standard deviation of the mean

TABLE II

TTS VS. ABSOLUTE PRESSURE AT CLAMPING

Coating 12MH

Samples Clamped at 75 cm. Hg Absolute Pressure		Samples Clamped at 8 cm. Hg Absolute Pressure	
Coat Weight, lb./ream	TTS, lb./in.^{2}	Coat Weight, lb./ream	TTS, lb./in.^{2}
14.5	1974	11.0	1310
17.0	1220	11.2	1375
15.6	1530	11.7	1305
14.3	1423	12.4	1410
13.4	1482	12.8	1248
14.5	1640	13.2	1483
11.5	1406	13.7	1468
13.1	1288	14.0	1308
14.0	1340	14.2	1308
		15.4	1332
av. 14.2	av. 1477	av. 13.0	av. 1350
σ_i[a] 1.8	σ_m[b] 74	σ_i 1.4	σ_m 24

[a] σ_i = standard deviation of the individual

[b] σ_m = standard deviation of the mean

TABLE III

TTS VS. RATE OF LOADING

Coating 12MA
Coat weight = 24±1 lb./ream

Rate of loading, lb./min.	100	500	1000
TTS, lb./in.^{2}	2280	2340	2418
	2480	2288	2510
			2420
av.	2380	2314	2449
σ_m	100	26	31

over-all av. = 2391 lb./in.^{2}

TABLE IV

COATING REPRODUCIBILITY

Coating 12MA

Color No. E-5807		Color No. E-5901	
Coat Weight, lb./ream	TTS, lb./in.^{2}	Coat Weight, lb./ream	TTS, lb./in.^{2}
26.4	2430	16.4	2243
27.8	2555	18.0	2430
29.0	2330	18.0	2293
29.3	2415	18.0	2245
29.4	2560	18.6	1993
29.6	2380	18.8	2168
30.5	2420	20.2	2278
30.9	2385	20.7	2390
31.1	2290	21.2	2140
32.4	2445	22.0	2318
32.4	2070	22.8	2103
		24.4	2100
av. 29.9	av. 2390	av. 19.9	av. 2225
σ_i 1.6	σ_m 74	σ_i 2.4	σ_m 37

TABLE V

TTS OF COATINGS ON "MF"

Coating 10MV

Penetration[a] = 0.2 lb./ream		Penetration = 2.2 lb./ream	
Failure near air or substrate surfaces		Failure in broad zone near center of coating on air side	
Coat Weight, lb./ream	TTS, lb./in.^{2}	Coat Weight, lb./ream	TTS, lb./in.^{2}
21.2	1630	21.5	1782
21.5	1590	21.8	1870
23.4	1818	22.6	1890
23.9	1625	22.8	1895
23.9	1768	23.4	1900
23.9	1823	23.4	1927
28.2	1803	25.2	1870
28.2	1660	25.8	1870
28.2	1697	27.1	1835
28.2	1762	29.0	1850
30.0	1626	29.8	1782
32.9	1718	30.5	1991
av. 26.1	av. 1710	av. 25.2	av. 1872
σ_i 3.6	σ_m 24	σ_i 3.2	σ_m 17

[a] Penetration of epoxy adhesive into the coating specimens.

TABLE V (Continued)

Coating 12SV

Penetration = (negligible)

Failure near substrate or random

Coat Weight, lb./ream	TTS, lb./in.^{2}
23.6	1762
24.0	1687
24.9	1803
25.0	1574
25.7	1742
26.5	1580
av. 25.0	av. 1691
σ_i 1.2	σ_m 39

Penetration = 0.4 lb./ream

Failure mostly random

Coat Weight, lb./ream	TTS, lb./in.^{2}
19.1	2155
19.4	2220
19.6	2073
20.4	2230
21.8	2155
22.8	2190
23.4	2238
23.9	2160
23.9	2190
24.4	2263
25.5	2038
27.4	2303
av. 22.6	av. 2185
σ_i 2.6	σ_m 22

Penetration = 0.0 lb./ream

Failure near substrate or random

Coat Weight, lb./ream	TTS, lb./in.^{2}
23.1	1850
23.6	1835
25.5	1987
26.0	1482
26.3	1559
av. 24.9	av. 1743
σ_i 1.4	σ_m 95

TABLE V (Continued)

Coating 12MV

Penetration = <1 lb./ream

Failure near substrate or random

Coat Weight, lb./ream	TTS, lb./in.^{2}
17.0	1853
20.3	1523
20.7	1857
21.6	1665
22.5	1670
22.7	1600
23.3	1900
23.5	1803
23.9	1742
25.0	1692
25.4	1872
26.3	1863
26.8	1790
28.5	1788
av. 23.5	av. 1759
σ_i 3.0	σ_m 30

Penetration = 3.4 lb./ream

Failure near substrate or random

Coat Weight, lb./ream	TTS, lb./in.^{2}
22.3	1890
23.1	1897
23.4	2013
23.6	2050
24.1	1972
24.7	2002
24.9	1830
26.5	1886
27.1	1860
30.5	1912
32.6	2052
36.6	1962
av. 26.6	av. 1944
σ_i 4.4	σ_m 44

TABLE V (Continued)

Coating 12LV

Penetration = <0.7 lb./ream

Failure 19.8% of coat wt. from substrate

Coat Weight, lb./ream	TTS, lb./in.^{2}
21.0	1182
22.8	1167
23.1	1192
23.1	1274
23.3	1167
23.6	1125
24.1	1370
24.7	926
25.2	1360
26.0	1070
av. 23.7	av. 1183
σ_i 1.4	σ_m 42

Penetration = 3.4 lb./ream

Failure 35.7% of coat wt. from substrate

Coat Weight, lb./ream	TTS, lb./in.^{2}
21.2	1590
21.2	1538
22.8	1498
23.1	1773
24.4	1702
24.4	1498
25.0	1671
25.0	1538
25.5	1595
25.8	1748
av. 23.8	av. 1615
σ_i 1.7	σ_m 32.3

TABLE V (Continued)

Coating 12SH

Penetration = 3.1 lb./ream

Failure adjacent to substrate

Coat Weight, lb./ream	TTS, lb./in.^{2}
21.8	1303
22.9	1325
23.9	1283
24.2	1355
25.0	1417
av. 23.6	av. 1335
σ_i 1.6	σ_m 21

Penetration = 3.7 lb./ream

Failure 72.7% of coat wt. from substrate

Coat Weight, lb./ream	TTS, lb./in.^{2}
20.4	2313
21.0	2280
21.0	2218
22.3	2267
22.3	2117
22.3	2066
23.1	2210
23.4	2295
23.9	2330
24.2	2230
24.4	2140
24.7	2226
av. 22.7	av. 2227
σ_i 1.4	σ_m 20

TABLE V (Continued)

Coating 12MH

Penetration = <1.1 lb./ream

Failure adjacent to substrate

Coat Weight, lb./ream	TTS, lb./in.^{2}
20.2	1202
20.4	1110
20.9	792
21.7	1074
21.8	1163
21.8	994
22.9	805
22.9	911
av. 21.6	av. 1006
σ_i 1.6	σ_m 56

Penetration = 1 lb./ream

Failure adjacent to substrate

Coat Weight, lb./ream	TTS, lb./in.^{2}
19.3	1515
19.3	1396
21.0	1365
26.7	1370
28.2	1280
28.9	1253
33.7	1342
av. 25.3	av. 1360
σ_i 5.6	σ_m 32

Penetration = 4.8 lb./ream (3 surfaces)[a]

Failure no. 1 near substrate; no. 2 partly near sub. and partly about 1/3 coat wt. from air surface

Coat Weight, lb./ream	TTS Failure no. 1, lb./in.^{2}	TTS Failure no. 2, lb./in.^{2}
20.3	1725	1730
20.7	1580	--
21.2	1565	2014
22.2	1677	1980
23.3	1603	2320
24.4	1913	--
av. 22.0	av. 1677	av. 2011
σ_i 1.6	σ_m 53	σ_m 121

[a] Each sample of coating was tested for TTS; the portion of coating on the air-surface side of failure no. 1 was retested, giving the TTS of failure no. 2.

TABLE V (Continued)

Coating 12LH

Penetration = 1.2 lb./ream

Failure 8.8% of coat wt. from substrate

Coat weight, lb./ream	TTS, lb./in.^{2}
20.0	1222
20.7	1375
21.0	1386
21.3	1462
21.8	1615
21.9	1645
21.9	1232
22.1	1325
22.3	1390
23.4	1563
av. 21.6	av. 1421
σ_i 0.8	σ_m 47

Penetration = 3.0 lb./ream

Failure 14.1% of coat wt. from substrate

Coat Weight, lb./ream	TTS, lb./in.^{2}
19.4	1600
20.7	1600
21.0	1926
21.0	1880
22.3	1916
22.6	1834
22.8	1742
22.8	1977
23.1	1783
23.6	1650
av. 21.9	av. 1788
σ_i 1.3	σ_m 43

TABLE V (Continued)

Coating 12SA

Penetration = 3.2 lb./ream

Failure near sub.

Coat Weight, lb./ream	TTS, lb./in.^{2}
20.7	1137
22.6	1462
23.1	1355
23.1	937
23.1	1157
23.1	1034
23.3	1222
23.6	1055
24.7	1172
24.9	978
25.5	1540
25.7	1070
av. 23.6	av. 1172
σ_i 1.4	σ_m 44

Penetration = 3.7 lb./ream

Failure 73.4% of coat wt. from sub.

Coat Weight, lb./ream	TTS, lb./in.^{2}
23.9	2287
23.9	2555
24.2	2523
24.4	2460
24.7	2565
25.2	2510
25.7	2338
26.0	2088
27.1	2560
27.6	2403
28.2	2422
29.2	2292
av. 25.8	av. 2417
σ_i 1.8	σ_m 42

TABLE V (Continued)

Coating 12MA

Penetration = < 4 lb./ream

Failure near surfaces

Coat Weight, lb./ream	TTS, lb./in.^{2}
15.1	1913
15.2	2270
16.0	1737
17.4	2050
18.8	1552
19.3	1500
19.8	1447
21.7	1308
21.9	1485
22.0	1463
22.1	1390
22.1	1930
25.6	1516
av. 19.8	av. 1659
σ_i 3.2	σ_m 82

Penetration = 4.3 lb./ream

Failure 77.7% of coat wt. from substrate

Coat Weight, lb./ream	TTS, lb./in.^{2}
16.4	2243
18.0	2430
18.0	2294
18.0	2245
18.6	1993
18.8	2168
20.2	2278
20.7	2390
21.2	2140
22.0	2318
22.8	2103
24.4	2100
av. 19.9	av. 2225
σ_i 2.4	σ_m 37

TABLE V (Continued)

Coating 12LA

Penetration = (negligible)

Failure 12.7% of coat wt. from substrate

Coat Weight, lb./ream	TTS, lb./in.^{2}
20.2	1580
21.8	1830
21.8	1560
22.3	1656
22.6	1635
22.6	1600
22.8	1645
23.6	1355
23.9	1670
24.2	1800
24.4	1564
av. 22.7	av. 1627
σ_i 1.2	σ_m 35

Penetration = 6.4 lb./ream

Failure 24.1% of coat wt. from substrate

Coat Weight, lb./ream	TTS, lb./in.^{2}
22.3	2252
23.1	2192
23.4	2168
24.2	2142
24.7	2163
25.5	2052
26.0	2163
26.5	2083
26.8	2214
27.9	2190
28.2	2047
31.9	2192
av. 25.9	av. 2155
σ_i 2.7	σ_m 18.4

TABLE V (Continued)

Coating 14MV

Penetration = 0.8 lb./ream

Failure near surfaces

Coat Weight, lb./ream	TTS, lb./in.^{2}
19.9	2278
22.0	2092
22.3	2140
22.5	2042
23.1	2176
23.9	2142
24.4	2033
24.4	2150
25.5	2267
25.7	2340
av. 23.4	av. 2166
σ_i 1.7	σ_m 32

Penetration = 2.1 lb./ream

Failure random

Coat Weight, lb./ream	TTS, lb./in.^{2}
20.7	2126
22.0	2308
22.5	2242
22.5	2318
23.1	2100
23.3	2136
23.3	2340
23.9	2384
24.4	2332
23.9	2178
24.4	2332
25.5	2370
av. 23.3	av. 2264
σ_i 1.3	σ_m 29.6

TABLE V (Continued)

Coating $14MV_{HAB}$

Penetration = 0.3 lb./ream

Failure 16.8% of coat wt. from substrate

Coat Weight, lb./ream	TTS, lb./in.^{2}
19.4	2001
20.4	1896
21.2	1762
21.2	2180
22.3	2205
22.3	2104
22.3	2078
23.6	2165
23.9	1824
23.9	2084
24.4	1900
24.7	2078
av. 22.4	av. 2023
σ_i 1.7	σ_m 42.3

Penetration = 0.7 lb./ream

Failure 14.2% of coat wt. from substrate

Coat Weight, lb./ream	TTS, lb./in.^{2}
19.4	1998
19.4	1998
19.6	2054
21.2	2067
21.2	2170
21.5	1922
22.3	1875
24.9	2144
25.7	2110
26.5	1895
27.3	2144
av. 22.6	av. 2034
σ_i 2.95	σ_m 31.6

TABLE VI

TTS OF COATINGS ON ALUMINUM FOIL

Coating	10MF	12SF	12MF[a]	12LF	14MF	$14MF_{HAB}$
Average coat wt., lb./ream	28	28	16[b]	27	24	31
TTS, lb./in.^{2}	1660	2136	868	1937	2110	871
	1417	2220	1010	2090	2017	367
	1513	1967	1103	2002	1860	367
	1488	2130	1617	2144	1844	1009
	1202	1758	1790	2190	2068	--
	1529	2144	2040	--	2073	--
	1407	--	--	--	2270	--
	968	--	--	--	2220	--
	1687	--	--	--	--	--
av.	1430	2059	1405	2072	2058	654
σ_m	75	69	194	46	44	170
Location of failure in coating	random	random	--[c]	random	random	near foil

[a] This coating was dried at less than 10% relative humidity; the other coatings except $14MF_{HAB}$ were dried at 50% relative humidity.

[b] The samples of this coating varied very much in coat weight, from about 10 to about 30 lb./ream.

[c] Thin coatings failed randomly and thick coatings failed near the foil-coating interface.

APPENDIX V

CALIBRATION DATA FOR STAYCO M STARCH

Colorimetric Method Using Iodine

Run No. 1		Run No. 2	
Starch, mg.	Optical Density	Starch, mg.	Optical Density
0.79	0.155	1.59	0.321
1.58	0.308	1.59	0.315
2.38	0.477	2.39	0.498
3.17	0.678	2.39	0.486
3.96	0.802	3.98	0.851
4.00	0.854	3.98	0.833

APPENDIX VI

ADHESIVE RATIO DATA

Adhesive Ratios of Coatings on Kodapak

Coating	10MK	12SK	12LK	14MK
Adhesive ratio	9.77	12.07	12.30	13.72
	9.90	11.92	12.60	13.52
	9.67	11.92	11.99	13.48
	9.87	12.00	12.16	13.58
av.	9.80	11.98	12.26	13.58
σ_m	0.05	0.04	0.13	0.03

Net Adhesive Ratios of Coatings on "MF"

Coating	10MV	12SV	12MV	12LV	14MV	$14MV_{HAB}$
Net adhesive ratio	8.22	9.75	9.57	9.75	11.22	12.59
	8.02	9.85	9.42	10.10	11.16	12.18
	8.03	9.88	9.41	9.46	11.21	12.25
	7.97	9.82	9.44	9.70	11.50	12.51
av.	8.06	9.82	9.46	9.75	11.27	12.38
σ_m	0.06	0.03	0.04	0.13	0.08	0.11

Coating	12SH	12MH	12LH	12SA	12MA	12LA
Net adhesive ratio	10.94	10.40	11.90	11.30	11.40	11.24
	11.02	10.93	11.48	11.22	11.21	11.47
	11.01	10.84	10.77	11.18	11.09	11.08
	—	10.71	11.30	11.68	11.07	11.80
av.	10.99	10.72	11.36	11.34	11.19	11.40
σ_m	0.03	0.12	0.23	0.13	0.08	0.17

APPENDIX VII

CALCULATION OF TIME REQUIRED FOR COATING TO SET

Calculation of time required for enough vehicle to leave the coating to cause the coating to set, using % $voids_{H_2O}$ data of Cobb (40):

Clay M (this study) had a specific surface = 14.04 $m.^2/g.$

Clay D_2 (Cobb's study) had a specific surface = 14.50 $m.^2/g.$

Therefore, the % $voids_{H_2O}$ of clay D_2 (55.0) will be used for clay M.

For a 55.0% solids coating with an adhesive ratio of 12 -- (basis = 100 g. clay)

	Weight, g.	Density, $g./cm.^3$	Volume, $cm.^3$
Clay	100	2.58	38.8
Starch	12	1.50	8.0
Water	91.6	1.00	91.6
Total	--	--	138.6

$$\% \text{ voids}_{H_2O} = 55.0 = (100\ V_{H_2O})/(38.8 + V_{H_2O})$$

V_{H_2O} = 47.4 $cm.^3$, volume of water to just fill the voids in the clay

Total vehicle vol. = 99.6 $cm.^3$

Vehicle volume that must be removed to set coating (neglecting the effects of the starch) = 52.2 $cm.^3/100$ g. clay.

For a coat weight of 20 lb./ream (2.96 $mg./cm^2$) 100 g. clay is distributed over 3.8×10^4 $cm.^2$.

Depth of vehicle penetration to set coating, $\underline{L}$, is --

$$\underline{L} = (52.4)/[(0.80)(3.8\times10^{4})] = 17.2 \text{ mu}$$

where 0.80 is the void fraction of the substrate

Time required for coating to set, $\underline{t}$, is --

$$\underline{t} = (2\eta\underline{L}^{2})/(\underline{r}\gamma\cos\theta)$$

where η = viscosity of vehicle migrating into substrate, poise

γ = surface free energy of vehicle, g./cm.

$\underline{r}$ = av. pore radius in substrate, cm.

θ = contact angle of vehicle against substrate, radians

For the above coating on "MF", type AA --

$$\underline{t} = [(2)(1)(1.72\times10^{-3})^{2}(980)]/[(0.4\times10^{-4})(50)(1)]$$

$$= 3.0 \text{ sec.}$$

For the same coating on "MF", type VC --

$$\underline{t} = 24 \text{ sec.}$$

In the above setting-time calculations it is assumed that:

η = 1 poise

θ = 0 radians

γ = 50 dynes/cm.